Published for SISSA by Springer

Received: May 4, 2022
Accepted: June 6, 2022
Published: July 13, 2022

Master integrals for mixed QCD-QED corrections to charged-current Drell-Yan production of a massive charged lepton

Ming-Ming Long, Ren-You Zhang, Wen-Gan Ma, Yi Jiang, Liang Han, Zhe Li and Shuai-Shuai Wang

State Key Laboratory of Particle Detection and Electronics,
University of Science and Technology of China,
Hefei 230026, Anhui, People's Republic of China
Department of Modern Physics, University of Science and Technology of China,
Hefei 230026, Anhui, People's Republic of China

E-mail: heplmm@mail.ustc.edu.cn, zhangry@ustc.edu.cn, mawg@ustc.edu.cn, jiangyi@ustc.edu.cn, hanl@ustc.edu.cn, brucelee@mail.ustc.edu.cn, wang1996@mail.ustc.edu.cn

Abstract: The master integrals for the mixed QCD-QED two-loop virtual corrections to the charged-current Drell-Yan process $q\bar{q}' \to \ell\nu$ are computed analytically by using the differential equation method. A suitable choice of master integrals makes it successful to cast the differential equation system into the canonical form. We keep the dependence on charged lepton mass in the building of differential equations and then expand the system against the ratio of small charged lepton mass to large W-boson mass. In such a way the final results will contain large logarithms of the form $\log(m_\ell^2/m_W^2)$. Finally, all the canonical master integrals are given as Taylor series around $d = 4$ spacetime dimensions up to order four, with coefficients expressed in terms of Goncharov polylogarithms up to weight four.

Keywords: Higher Order Electroweak Calculations, Higher-Order Perturbative Calculations

ArXiv ePrint: 2111.14130

https://doi.org/10.1007/JHEP07(2022)078

JHEP07(2022)078

Contents

1 Introduction

With decades of accumulation of diligent investigations from both experimental and theoretical communities, the Drell-Yan (DY) processes [1] have become one of the best understood physics subjects at the LHC. They provide an excellent environment to probe the inner structure of proton [2] and the nature of the electroweak (EW) sector of the Standard Model (SM) by precision measurements of many EW observables, such as W-boson mass and width [3, 4], Weinberg weak mixing angle [5, 6] and charge asymmetries [7, 8]. These are built on the huge amount of event data collected at colliders thanks to the large cross sections and clean experimental signatures of DY processes. In addition to the precision test of the SM, DY processes could help to search for signals of new physics as well because the new vector bosons predicted by conjectured extensions of the SM can be produced by a similar mechanism [9–15]. Precision measurements of DY processes must be confronted with equally precise theoretical predictions, therefore the theoretical perturbative descriptions of DY processes should be extended to higher orders.

At the parton level, the DY processes at the lowest-order can be categorized into neutral-current processes ($q\bar{q} \to \gamma/Z \to \ell^+\ell^-$) and charged-current processes ($q\bar{q}' \to W \to \ell\nu$). The production rates of those DY processes were computed up to the QCD next-to-next-to-leading order (NNLO) decades ago [16–19], which turned out to be a great

JHEP07(2022)078

triumph in precision study of phenomenology of particle physics. In refs. [20–24], W and Z productions in hadron collisions were studied fully differentially at NNLO in QCD. The threshold corrections to DY production at N^{3}LO in QCD were presented in refs. [25, 26]. Recently, progress has been made toward N^{3}LO at the inclusive level for both neutral- and charged-current DY processes [27–29]. At the differential level, the transverse-momentum and rapidity distributions of DY lepton pair at N^{3}LO in α_s were calculated in refs. [30] and [31], respectively. Due to the leptonic final state of DY processes, the QCD corrections are only involved in the initial state. However, the EW radiative corrections are more complicated; they cannot be fully factorized into the corrections to the production and decay of the intermediate gauge boson separately. The NLO EW corrections to the neutral- and charged-current DY processes have been studied in refs. [32–38] and [39–45], respectively. A fully differential description of NLO corrections to DY processes has been implemented in automated Monte Carlo (MC) programs. For a review on QCD and EW radiative corrections to W- and Z-boson observables, see ref. [46]. The authors presented a systematic comparison of a dozen MC codes, which served as either a general MC framework or a dedicated program for (partial) DY processes. There are also some implementations at QCD NNLO, such as `GENEVA` [47, 48], `DYTurbo` (improved reimplementation of `DYqT`, `DYRes`, `DYNNLO`) [49], `MCFM` [50], `MATRIX` [51] and `MiNNLO`$_{\texttt{PS}}$ [52]. A comparison of those NNLO MC generators was provided in ref. [53] very recently.

To build an exhaustive comprehension of DY processes at NNLO, it is necessary to consider the mixed QCD-EW corrections which are not yet available. The mixed QCD-EW NNLO corrections to DY processes can be divided into two categories: factorizable and non-factorizable. For Z-boson production in hadron collisions, the mixed QCD-QED corrections have been studied at both inclusive and exclusive levels in refs. [54–56], and the mixed QCD-EW corrections are given in refs. [57–59]. As for W-boson production, the mixed QCD-EW corrections can be found in ref. [60]. The radiative corrections of $\mathcal{O}(N_f\alpha_s\alpha)$ to off-shell W/Z production at the LHC are also provided in ref. [61]. The non-factorizable initial-final corrections to DY processes in the resonance region can be estimated via the so-called pole approximation [62, 63]. The full NNLO mixed QCD-EW corrections to $pp \to \ell\nu + X$ at the LHC were given in ref. [64], where the two-loop virtual corrections are computed in the pole approximation while the rest contributions are calculated without any approximation. In the precision calculation of the non-factorizable mixed QCD-EW corrections, the primary technical problem is the evaluation of massive two-loop four-point master integrals (MIs) induced by the most complicated box-type Feynman diagrams. The two-loop box-type MIs have been calculated analytically and numerically in the approximation of $m_W = m_Z$ and $m_\ell = 0$ [65–67]. Recently, the mixed QCD-EW two-loop scattering amplitude for $q\bar{q} \to \ell^+\ell^-$ in dimensional regularization and its independence on γ^5 scheme were studied in detail in refs. [68, 69], and the complete mixed QCD-EW NNLO corrections to the DY production of a massless lepton pair were first computed in refs. [70, 71].

When lepton mass is taken into consideration, the collinear photon emission off the final-state charged lepton(s) gives rise to the radiative corrections that are enhanced by large logarithms of the form $\log(m_\ell^2/Q^2)$, where Q stands for a characteristic scale of DY processes, like weak gauge boson mass or center-of-mass colliding energy. As is well

JHEP07(2022)078

known, those logarithms cancel exactly if collinear lepton-photon systems are treated fully inclusively, which is guaranteed by the Kinoshita-Lee-Nauenberg theorem [72, 73]. In the presence of phase-space cuts and in kinematic distributions, in general, the mass-singular contributions survive, but the collinear safety can be restored after performing the photon recombination procedure [40–42, 45]. Those mass-singular contributions can be fully captured by considering only the QED part of the EW corrections, since they are only induced by collinear photon radiation from charged leptons. The analytic calculation of the MIs for the mixed QCD-QED corrections to DY production of a massive lepton pair has been accomplished [74]. In this paper we focus on the charged-current DY process $q\bar{q}' \to \ell\nu$ with non-zero lepton mass, and calculate the MIs for the mixed QCD-QED two-loop virtual corrections.

The rest of this paper is organized as follows. In section 2 the notation and conventions are declared. In section 3, the canonical differential equations are constructed, and the 46 canonical MIs for the mixed QCD-QED two-loop virtual corrections to $q\bar{q}' \to \ell\nu$ are evaluated analytically. Finally, a short summary is given in section 4.

2 Notation and conventions

In this paper we study the charged-current DY process

$$q(p_1) + \bar{q}'(p_2) \to \ell(p_3) + \nu(p_4)\,. \tag{2.1}$$

The light quarks are considered as massless while the charged lepton mass is kept non-zero throughout our calculation. All the external particles are on their mass-shell, i.e., $p_1^2 = p_2^2 = p_4^2 = 0$ and $p_3^2 = m_\ell^2$, and the scattering amplitude can be expressed in terms of the Mandelstam invariants

$$s = (p_1 + p_2)^2\,, \qquad t = (p_2 - p_3)^2\,, \qquad u = (p_1 - p_3)^2\,, \tag{2.2}$$

which satisfy $s + t + u = m_\ell^2$ due to momentum conservation. The mixed QCD-QED two-loop virtual corrections to $q\bar{q}' \to \ell\nu$ can be classified as follows:

- *Non-factorizable corrections*

  All the non-factorizable mixed QCD-QED two-loop Feynman diagrams are box type and irreducible. The dimensionally regularized two-loop four-point Feynman integrals in $d = 4 - 2\epsilon$ dimensions have the form as

  $$F(n_1, \ldots, n_9) = \int \mathcal{D}^d l_1 \mathcal{D}^d l_2 \frac{1}{D_1^{n_1} \ldots D_9^{n_9}}\,, \qquad (n_i \in \mathbb{Z}, \quad i = 1, \ldots, 9)\,, \tag{2.3}$$

  where $l_{1,2}$ are loop momenta and the integration measure is defined by

  $$\mathcal{D}^d l_i = \frac{d^d l_i}{(2\pi)^d} \left(\frac{i S_\epsilon}{16\pi^2}\right)^{-1} \quad \text{with} \quad S_\epsilon = (4\pi)^\epsilon \frac{\Gamma(1+\epsilon)\Gamma(1-\epsilon)^2}{\Gamma(1-2\epsilon)}\,. \tag{2.4}$$

  For arbitrary $n_i \in \mathbb{Z}$, $i = 1, \ldots, 9$, the set of all such $F(n_1, \ldots, n_9)$ in eq. (2.3) is called an integral family. For an integral $F(n_1, \ldots, n_9)$, we defined its sector as $[s_1, \ldots, s_9]$

JHEP07(2022)078

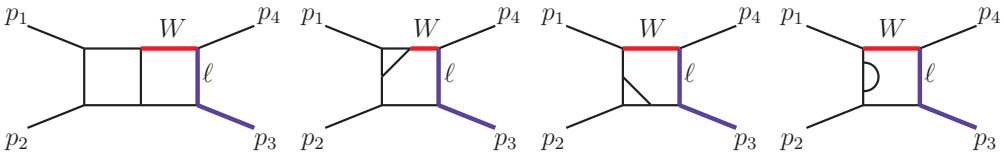

Figure 1. Four topologies of Feynman diagrams for non-factorizable mixed QCD-QED two-loop virtual corrections to $q\bar{q}' \to \ell\nu$. All the diagrams in this paper are drawn by using `JaxoDraw` [75].

with $s_i = \Theta(n_i - 1/2)$.[1] These non-factorizable box-type two-loop Feynman diagrams can be categorized into 8 topologies. The 4 topologies shown in figure 1 belong to the integral family $\mathcal{F}$, which is identified by the set of propagators

$$\begin{aligned} &D_1 = l_1^2\,, && D_2 = (l_1+p_1)^2 - m_W^2\,, && D_3 = (l_1-p_2)^2\,, \\ &D_4 = l_2^2\,, && D_5 = (l_2+p_1)^2\,, && D_6 = (l_2-p_2)^2\,, \\ &D_7 = (l_1-l_2)^2\,, && D_8 = (l_1-p_2+p_3)^2 - m_\ell^2\,, && D_9 = (l_2-p_2+p_3)^2\,, \end{aligned} \tag{2.5}$$

while the other 4 topologies can be obtained from figure 1 by exchanging p_1 and p_2 and thus belong to the family $\mathcal{F}^* \equiv \mathcal{F}\big|_{p_1 \leftrightarrow p_2}$. The MIs for the non-factorizable mixed QCD-QED two-loop virtual corrections to $q\bar{q}' \to \ell\nu$ will be computed analytically in section 3.

- *Factorizable corrections*

  There are totally 24 factorizable Feynman diagrams for the mixed QCD-QED two-loop virtual corrections to $q\bar{q}' \to \ell\nu$. Four of them are reducible and can be evaluated analytically by using the techniques for one-loop integrals. The rest 20 Feynman diagrams are irreducible and can be regarded as the mixed QCD-QED two-loop virtual corrections to $q\bar{q}' \to W^*$. These two-loop three-point Feynman diagrams can be categorized into 8 topologies which belong to 3 different integral families. A detailed discussion on the MIs for the mixed QCD-QED two-loop virtual corrections to $q\bar{q}' \to W^*$ is given in appendix A.

3 Non-factorizable mixed QCD-QED virtual corrections to $q\bar{q}' \to \ell\nu$

As stated in section 2, the 8 non-factorizable two-loop Feynman diagrams for the mixed QCD-QED virtual corrections to $q\bar{q}' \to \ell\nu$ are categorized into 8 topologies respectively, which belong to 2 integral families. Due to the fact that the 4 topologies/diagrams belonging to $\mathcal{F}^*$ can be obtained from the corresponding ones belonging to $\mathcal{F}$ by exchanging p_1 and p_2, only the 4 topologies in figure 1 are considered in the following discussion.

[1] The concept of sector is equivalent to the topology of Feynman diagrams, and thus we do not distinguish between sector and topology in this paper.

JHEP07(2022)078

The 4 topologies in figure 1 belong to the integral family $\mathcal{F}$, corresponding to the following 4 sectors of $\mathcal{F}$, respectively,

$$\begin{aligned}&[0,1,1,1,1,1,1,1,0]\,,\\&[1,1,1,1,1,0,1,1,0]\,,\\&[1,1,1,1,0,1,1,1,0]\,,\\&[1,1,1,1,0,0,1,1,0]\,.\end{aligned} \tag{3.1}$$

For a given sector $[s_1, s_2, \ldots]$, we define

$$[s_1, s_2, \ldots]_F = \bigcup_{s'_i \in \{0,1\} \text{ and } \leqslant s_i} [s'_1, s'_2, \ldots]\,. \tag{3.2}$$

The scalar integrals induced by a Feynman diagram (corresponding a tensor integral) of this sector/topology via tensor reduction belong to $[s_1, s_2, \ldots]_F$. Thus, the scalar integrals induced by the 4 topologies in figure 1 certainly belong to the following integral set,

$$\mathcal{S} = [0,1,1,1,1,1,1,1,0]_F \cup [1,1,1,1,1,0,1,1,0]_F \cup [1,1,1,1,0,1,1,1,0]_F\,. \tag{3.3}$$

We compute the MIs of $\mathcal{S}$ in the unphysical region, namely $s < 0, -m_W^2 < t < 0,\ m_\ell^2 > 0$ and $m_W^2 > 0$, where all the MIs are real-valued. Then their values in the physical region can be obtained by analytic continuation.

3.1 Canonical differential equations

In this section, we elaborate on the construction of canonical differential equations for the MIs and present the solution of the canonical differential system. The scalar Feynman integrals of a given family are not independent: there are integration-by-parts (IBP) recurrence relations [76]. After performing IBP reduction procedure, a minimal number of irreducible integrals which are also called master integrals are obtained; any dimensionally regularized scalar integral in this family can be expressed as a linear combination of the MIs with coefficients being the rational functions of kinematic variables and spacetime dimension. This is quite important for using the differential equation method [77, 78] to compute scalar Feynman integrals. In this work, we adopt `Kira` [79, 80] based on Laporta's algorithm [81] to perform IBP reduction, and then obtain 46 MIs, $f_{1,\ldots,46}$ of $\mathcal{S}$, which are depicted in figure 2.

The mass dimension of the scalar Feynman integral F in eq. (2.3) is given by

$$[F] = 2\,(d - \alpha) \qquad \text{with} \qquad \alpha = \sum_{i=1}^{9} \alpha_i\,. \tag{3.4}$$

Thus, F can be nondimensionalized by multiplying a factor of $Q^{-[F]}$, i.e.,

$$F \quad \longrightarrow \quad Q^{-[F]} \times F\,, \tag{3.5}$$

where Q is a characteristic mass scale. In this work, we take $Q = m_W$ and introduce the following three dimensionless variables for convenience,

$$x = -\frac{s}{m_W^2}\,, \qquad y = -\frac{t}{m_W^2}\,, \qquad z = \frac{m_\ell^2}{m_W^2}\,. \tag{3.6}$$

Then the nondimensionalized scalar Feynman integrals are functions of x, y and z.

JHEP07(2022)078

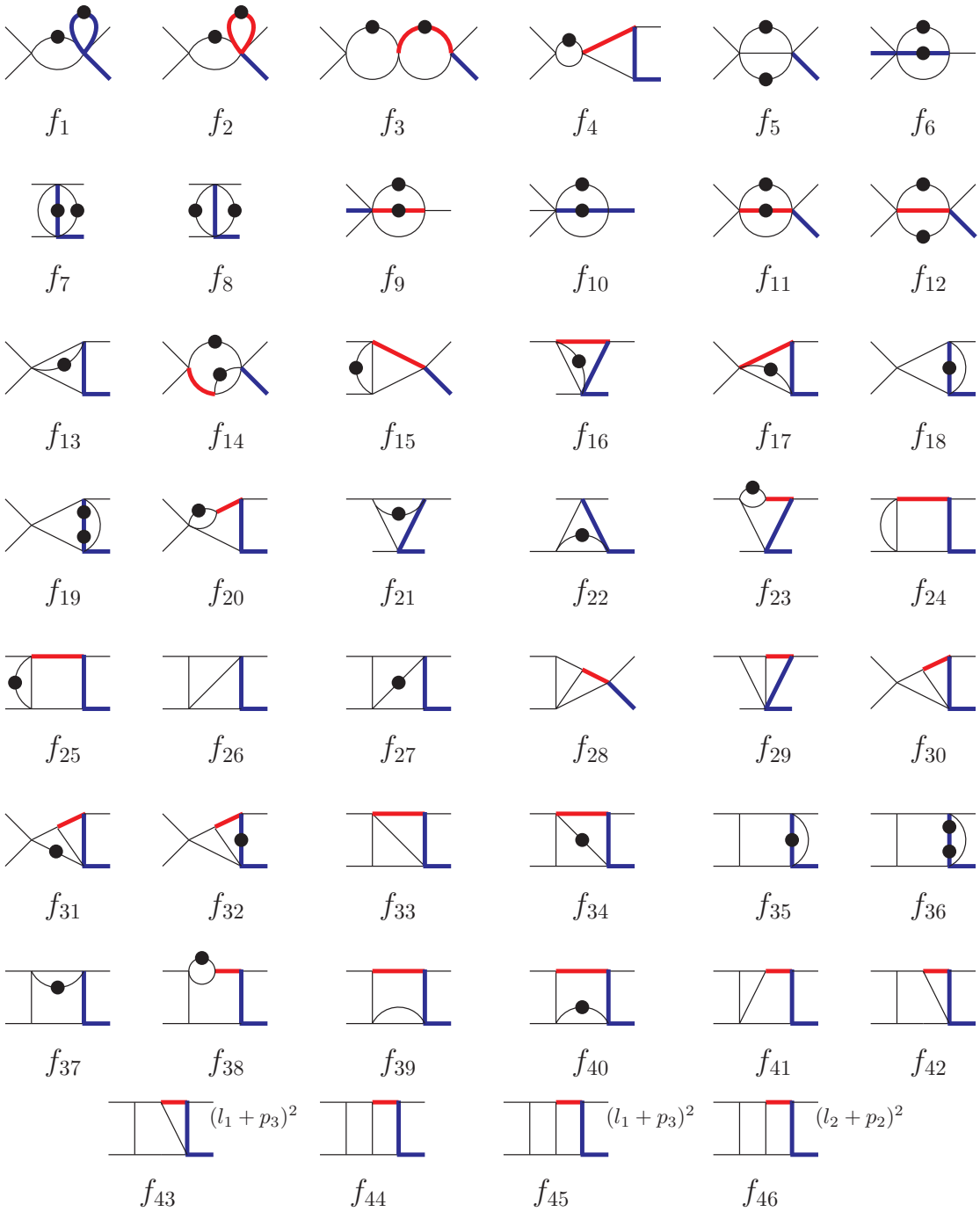

Figure 2. A set of pre-canonical MIs. The thin and thick lines represent massless and massive external particles and propagators respectively (red for W boson and blue for charged lepton). One dot means the index of that propagator is raised to 2 and two dots go for 3.

JHEP07(2022)078

With the help of `LiteRed` [82, 83], we obtain the partial derivatives of the 46 MIs with respect to x, y and z. By means of IBP identities, those derivatives are expressed as the linear combinations of the 46 MIs. This leads to the following set of partial differential equations for the vector of MIs $\mathbf{F} \equiv (f_1, f_2, \ldots, f_{46})^T$,

$$\frac{\partial \mathbf{F}}{\partial x} = \mathrm{A}_x(x,y,z;\epsilon)\,\mathbf{F}\,, \qquad \frac{\partial \mathbf{F}}{\partial y} = \mathrm{A}_y(x,y,z;\epsilon)\,\mathbf{F}\,, \qquad \frac{\partial \mathbf{F}}{\partial z} = \mathrm{A}_z(x,y,z;\epsilon)\,\mathbf{F}\,. \tag{3.7}$$

It was suggested in ref. [84] that a good choice of MIs would simplify the calculation tremendously. By means of the following basis transformation $\mathbb{T} : \mathbf{F} \longmapsto \mathbf{G}$

$$\begin{aligned}
g_1 &= \epsilon^2\, f_1\, x\,, & g_2 &= \epsilon^2\, f_2\, x\,,\\
g_3 &= \epsilon^2\, f_3\, x^2\,, & g_4 &= \epsilon^3\, f_4\, x\,(x+z)\,,\\
g_5 &= \epsilon^2\, f_5\, x\,, & g_6 &= \epsilon\,(1-\epsilon)\, f_6\, z\,,\\
g_7 &= \epsilon^2\, f_7\, y\,, & g_8 &= \epsilon^2\, f_8\,(y+z) + 2\,\epsilon^2\, f_7\, z\,,\\
g_9 &= \epsilon\,(1-\epsilon)\, f_9\,, & g_{10} &= \epsilon^2\, f_{10}\, z\,,\\
g_{11} &= \epsilon^2\, f_{11}\, x\,, & g_{12} &= \epsilon^2\, f_{12}\,(x+1) + 2\,\epsilon^2\, f_{11}\,,\\
g_{13} &= \epsilon^3\, f_{13}\,(x+z)\,, & & \\
g_{14} &= \left[\epsilon^2\, f_{14}\, x\,(x+1) + (1/2)\,\epsilon\,(1-\epsilon)\, f_9\, x + (3/2)\,\epsilon^2\, f_5\, x^2\right]/(1-x)\,, & &\\
g_{15} &= \epsilon^3\, f_{15}\, x\,, & g_{16} &= \epsilon^3\, f_{16}\, y\,,\\
g_{17} &= \epsilon^3\, f_{17}\,(x+z)\,, & g_{18} &= \epsilon^3\, f_{18}\,(x+z)\,,\\
g_{19} &= \epsilon^2\, f_{19}\, z\,(x+z)\,, & g_{20} &= \epsilon^3\, f_{20}\,(x+z)\,,\\
g_{21} &= \epsilon^3\, f_{21}\, y\,, & g_{22} &= \epsilon^3\, f_{22}\,(y+z)\,,\\
g_{23} &= \epsilon^3\, f_{23}\, y\,, & g_{24} &= \epsilon^3\,(1-2\epsilon)\, f_{24}\,(x+z)\,,\\
g_{25} &= \epsilon^3\, f_{25}\,(x+1)\,(y+z)\,, & g_{26} &= \epsilon^4\, f_{26}\,(x+y)\,,\\
g_{27} &= \epsilon^3\, f_{27}\, x\,(y+z)\,, & g_{28} &= \epsilon^4\, f_{28}\, x\,,\\
g_{29} &= \epsilon^4\, f_{29}\, y\,, & g_{30} &= \epsilon^4\, f_{30}\,(x+z)\,,\\
g_{31} &= \epsilon^3\, f_{31}\, x\,(x+z)\,, & g_{32} &= \epsilon^3\, f_{32}\,(1-z)\,(x+z)\,,\\
g_{33} &= \epsilon^4\, f_{33}\,(x+y+z)\,, & g_{34} &= \epsilon^3\, f_{34}\,(x+1)\,(y+z)\,,\\
g_{35} &= \epsilon^3\, f_{35}\, x\, y\,, & g_{36} &= \epsilon^2\,[\, f_{36}\,(y+z) + \epsilon\, f_{35}\,]\, x\, z\,,\\
g_{37} &= \epsilon^3\, f_{37}\, x\,(y+z)\,, & g_{38} &= \epsilon^3\,[\, f_{38}\,(x+1) + f_{37}\,]\,(y+z)\,,\\
g_{39} &= \epsilon^3\,(1-2\epsilon)\, f_{39}\, y\,, & g_{40} &= \epsilon^3\, f_{40}\,(x+1)\,(y+z)\,,\\
g_{41} &= \epsilon^4\, f_{41}\sqrt{\lambda}\,, & g_{42} &= \epsilon^4\, f_{42}\, x\, y\,,\\
g_{43} &= \epsilon^4\, f_{43}\, x - \epsilon^4\, f_{33}\,(2x+y+z)\,, & g_{44} &= \epsilon^4\, f_{44}\, x\,(x+1)\,(y+z)\,,\\
g_{45} &= \epsilon^4\,(f_{45}\, x - f_{44}\, x\, z + f_{41}\, y)\,(x+1)\,, & g_{46} &= \epsilon^4\, f_{46}\, x\,(x+z)\,,
\end{aligned} \tag{3.8}$$

we obtain a canonical set of MIs $\mathbf{G} = (g_1, g_2, \ldots, g_{46})^T$. Such a canonical basis $\mathbf{G}$ obeys the following system of differential equations,

$$\frac{\partial \mathbf{G}}{\partial x} = \epsilon\, \mathbb{A}_x(x,y,z)\,\mathbf{G}\,, \qquad \frac{\partial \mathbf{G}}{\partial y} = \epsilon\, \mathbb{A}_y(x,y,z)\,\mathbf{G}\,, \qquad \frac{\partial \mathbf{G}}{\partial z} = \epsilon\, \mathbb{A}_z(x,y,z)\,\mathbf{G}\,, \tag{3.9}$$

JHEP07(2022)078

where the dependence on the dimensional regularization parameter ϵ is completely factorized from the kinematics. Since the canonical differential system in eq. (3.9) is invariant under the scaling transformation $\mathbf{G} \longmapsto \epsilon^a \mathbf{G}$, the canonical basis $\mathbf{G}$ defined in eq. (3.8) has been required to be analytic and nonzero at $\epsilon = 0$. Finally, it is worth mentioning that all the entries of the basis transformation matrix $\mathbb{T}$ are rational functions of x, y and z, except

$$\mathbb{T}_{41,41} = \epsilon^4 \sqrt{\lambda} \qquad \text{with} \qquad \lambda = \left[x\,(y+z) + x + y\right]^2 - 4\,x^2\,z\,. \tag{3.10}$$

3.2 Integrations

The partial differential equations in eq. (3.9) can be combined into a $d\log$-form total differential equation,

$$d\mathbf{G} = \epsilon\, d\mathbb{A}\, \mathbf{G}\,, \qquad d\mathbb{A} = \sum_{i=1}^{15} \mathbb{C}_i\, d\log \eta_i\,, \tag{3.11}$$

where $\mathbb{C}_i$ $(i = 1, \ldots, 15)$ are constant matrices with rational-number entries, and the arguments of the $d\log$'s,

$$\begin{aligned}
&\eta_1 = x\,, && \eta_6 = x + y\,, && \eta_{11} = y + z + x\,z\,,\\
&\eta_2 = y\,, && \eta_7 = x + z\,, && \eta_{12} = \sqrt{\lambda}\,,\\
&\eta_3 = z\,, && \eta_8 = y + z\,, && \eta_{13} = x\,(y+z) + x + y + \sqrt{\lambda}\,,\\
&\eta_4 = 1 + x\,, && \eta_9 = x + y + z\,, && \eta_{14} = x\,(y+z) - x + y + \sqrt{\lambda}\,,\\
&\eta_5 = 1 - z\,, && \eta_{10} = 1 - y - z\,, && \eta_{15} = x\,(y+z) - x - y + \sqrt{\lambda}\,,
\end{aligned} \tag{3.12}$$

are called letters and together constitute the alphabet of our problem. Considering the mass hierarchy between W boson and charged lepton ($m_\ell \ll m_W$), we may expand the differential system for small z. After the expansion for small z, the coefficient matrix $d\mathbb{A}$ can be expressed as

$$d\mathbb{A} = \sum_{i=1}^{7} \widetilde{\mathbb{C}}_i\, d\log \alpha_i + d\left[\sum_{n=1}^{+\infty} \mathbb{A}_n(x,y)\, z^n\right]\,, \tag{3.13}$$

where

$$\begin{aligned}
&\alpha_1 = x\,, && \alpha_2 = 1 + x\,, && \alpha_3 = x + y\,,\\
&\alpha_4 = x + y + x\,y\,, && \alpha_5 = y\,, && \alpha_6 = 1 - y\,,\\
&\alpha_7 = z\,,
\end{aligned} \tag{3.14}$$

$$\begin{aligned}
&\widetilde{\mathbb{C}}_1 = \mathbb{C}_1 + \mathbb{C}_7 + \mathbb{C}_{15}\,, && \widetilde{\mathbb{C}}_2 = \mathbb{C}_4 + \mathbb{C}_{14}\,, && \widetilde{\mathbb{C}}_3 = \mathbb{C}_6 + \mathbb{C}_9\,,\\
&\widetilde{\mathbb{C}}_4 = \mathbb{C}_{12} + \mathbb{C}_{13}\,, && \widetilde{\mathbb{C}}_5 = \mathbb{C}_2 + \mathbb{C}_8 + \mathbb{C}_{11} + \mathbb{C}_{14} + \mathbb{C}_{15}\,, &&\\
&\widetilde{\mathbb{C}}_6 = \mathbb{C}_{10}\,, && \widetilde{\mathbb{C}}_7 = \mathbb{C}_3\,, &&
\end{aligned} \tag{3.15}$$

and $\mathbb{A}_n(x,y)$ $(n \in \mathbb{N}^+)$ are completely comprised of rational-function entries.[2] Therefore, the matrices $\mathbb{A}_{x,y}(x,y,z)$ and $\mathbb{A}_z(x,y,z)$ in eq. (3.9) are analytic and singular at $z = 0$,

[2] All the poles of $\mathbb{A}_n(x,y)$ $(n \in \mathbb{N}^+)$ are zeros of α_i $(i = 1, \ldots, 6)$.

JHEP07(2022)078

respectively, and can be expanded as

$$\begin{cases} \mathbb{A}_x(x,y,z) = \sum\limits_{n=0}^{+\infty} \mathbb{A}_{x,n}(x,y)\, z^n & \\ \mathbb{A}_y(x,y,z) = \sum\limits_{n=0}^{+\infty} \mathbb{A}_{y,n}(x,y)\, z^n & \text{(Taylor expansion)} \\ \mathbb{A}_z(x,y,z) = \dfrac{\mathbb{A}_{z,-1}}{z} + \sum\limits_{n=0}^{+\infty} \mathbb{A}_{z,n}(x,y)\, z^n & \text{(Laurent expansion)} \end{cases} \tag{3.16}$$

In the lowest-order approximation,

$$d\mathbb{A} \simeq \sum_{i=1}^{7} \widetilde{\mathbb{C}}_i\, d\log\alpha_i\,, \tag{3.17}$$

the 7 letters α_i $(i = 1,\ldots,7)$ constitute the alphabet of the differential system. As is well known, the leading terms in the z-expansion in eq. (3.16) ($\mathbb{A}_{x,0}$, $\mathbb{A}_{y,0}$ and $\mathbb{A}_{z,-1}$) are responsible for the logarithmic lepton-mass singularities of the canonical MIs $\mathbf{G}$. Thus, the logarithmically divergent contributions of the form $\log^n z$ can be fully captured by adopting the lowest-order approximation. In this work, we adopt the second-order approximation, i.e.,

$$d\mathbb{A} \simeq \sum_{i=1}^{7} \widetilde{\mathbb{C}}_i\, d\log\alpha_i + d\big[\mathbb{A}_1(x,y)\, z\big]\,, \tag{3.18}$$

in order to get the analytic expression for $\mathbf{G}$ up to $\mathcal{O}(z\log^n z)$. In the unphysical region,

$$x > 0 \;\wedge\; 0 < y < 1 \;\wedge\; z > 0\,, \tag{3.19}$$

α_i $(i = 1,\ldots,7)$ are real and positive. To evaluate the MIs in the physical region, the same analytic continuation procedure as in ref. [65] should be applied.

Since $\mathbf{G}$ is finite in the limit $\epsilon \to 0$, it can be expanded in a Taylor series around four dimensions,

$$\mathbf{G} = \sum_{n=0}^{\infty} \mathbf{G}^{(n)}\, \epsilon^n\,. \tag{3.20}$$

From eq. (3.9), one can establish the differential equations connecting $\mathbf{G}^{(n)}$ and $\mathbf{G}^{(n-1)}$. These first-order differential equations can be integrated in an iterative manner, namely order by order in ϵ. Then the canonical MIs at $\mathcal{O}(\epsilon^n)$ can be expressed as

$$\mathbf{G}^{(n)} = \sum_{m=0}^{n} \mathbb{M}^{(n-m)}\, \mathbf{C}^{(m)}\,, \tag{3.21}$$

where $\mathbf{C}^{(n)}$ is the integration constant vector at $\mathcal{O}(\epsilon^n)$ and the matrices $\mathbb{M}^{(n)}$ $(n \in \mathbb{N})$ are defined recursively by

$$\mathbb{M}^{(n)} = \mathbb{M}_x^{(n)} + \mathbb{M}_y^{(n)} + \mathbb{M}_z^{(n)}\,, \qquad \begin{cases} \mathbb{M}_x^{(n)} = \displaystyle\int \mathbb{A}_x\, \mathbb{M}^{(n-1)}\, dx & \\ \mathbb{M}_y^{(n)} = \displaystyle\int \Big(\mathbb{A}_y\, \mathbb{M}^{(n-1)} - \partial_y\, \mathbb{M}_x^{(n)}\Big)\, dy & \\ \mathbb{M}_z^{(n)} = \displaystyle\int \Big(\mathbb{A}_z\, \mathbb{M}^{(n-1)} - \partial_z\, \mathbb{M}_x^{(n)} - \partial_z\, \mathbb{M}_y^{(n)}\Big)\, dz & \end{cases} \tag{3.22}$$

JHEP07(2022)078

with $\mathbb{M}^{(0)} = \mathbf{1}$. Actually, it is sufficient to expand $\mathbf{G}$ up to the order of ϵ^4 for the mixed QCD-QED two-loop virtual corrections to charged-current DY processes. Since the entries of $\mathbb{A}_{x,y,z}$ are all rational functions of x, y and z after the expansion for small z, $\mathbb{M}^{(n)}$ can be expressed in terms of rational functions and Goncharov polylogarithms (GPLs) [85, 86]. A GPL with weights w_i $(i = 1, \ldots, n)$ and argument t is defined recursively by

$$G(w_n, \ldots, w_1; t) = \int_0^t \frac{1}{\tau - w_n} G(w_{n-1}, \ldots, w_1; \tau)\, d\tau \tag{3.23}$$

with $G(\,; t) = 1$ and

$$G\left(\vec{0}_n; t\right) = \frac{\log^n t}{n!}\,. \tag{3.24}$$

For the MIs $\mathbf{G}$ involved in the calculation of the non-factorizable mixed QCD-QED two-loop virtual corrections to $qq' \to \ell\nu$, the weights of the GPLs with arguments x, y and z are drawn from the following three sets, respectively,

$$\mathcal{W}_x = \left\{0,\, -1,\, -y,\, -\frac{y}{1+y}\right\}, \qquad \mathcal{W}_y = \{0,\, 1\}\,, \qquad \mathcal{W}_z = \{0\}\,. \tag{3.25}$$

In the recursive definition for $\mathbb{M}^{(n)}$ in eq. (3.22), one encounters the integrals with integrands of the form $r(t)\, G(\vec{w}; t)$, where $r(t)$ and $G(\vec{w}; t)$ represent rational functions and GPLs, respectively. Those integrals can be calculated recursively by using the following IBP recurrence relation,

$$\int_0^t r(\tau)\, G(\vec{w}_n; \tau)\, d\tau = \Big[R(\tau)\, G(\vec{w}_n; \tau)\Big]_0^t - \int_0^t R(\tau)\, \frac{1}{\tau - w_n}\, G(\vec{w}_{n-1}; \tau)\, d\tau\,, \tag{3.26}$$

where $\vec{w}_n = (w_n, \ldots, w_1)$, $\vec{w}_{n-1} = (w_{n-1}, \ldots, w_1)$, and $R(t)$ is an antiderivative of $r(t)$. In this paper we employ the `Mathematica` package `PolyLogTools` [87–89] and `C++` library `GiNaC` [90] for both symbolic computation and numerical evaluation [91] of GPLs.

3.3 Boundary conditions

To obtain the exact solution of the canonical differential system in eq. (3.9), the integration constants (i.e., the boundary terms of the MIs $g_{1,\ldots,46}$) have to be specified. For some of the MIs, we take their known analytic solutions from the literature or evaluate them by means of some much simpler differential systems. For all other MIs, the boundary terms are fixed by imposing a set of regularity conditions, i.e., demanding regularity of those MIs or their linear combinations in certain kinematic limits. It was found that the weight structure of integration constants in ref. [74] is quite simple. The integration constants at $\mathcal{O}(\epsilon^n)$ $(n = 0, 1, 2, 3, 4)$ are proportional to 1, 0, $\zeta(2)$, $\zeta(3)$ and $\zeta(4)$, respectively. This property still holds in our case. For our problem, the conditions imposed to the MIs for the determination of their boundary constants are listed below.

- $g_{1,2,3,5,\ldots,12,14,15,22,28}$ are taken from refs. [65, 74] as independent input.
- $g_{13,18}$ are determined by matching against the MIs with full lepton mass dependence, which are computed in appendix B.

JHEP07(2022)078

- The boundary constants of the rest 29 MIs are fixed by the following linearly independent regularity conditions:[3]

  - regularity at $x \to 0$: $g_{4,17,24,25,30,31,34,40,46}$
  - regularity at $x \to -y$: $g_{26,27,33,35,36,37,38,40,41,42,43,44}$
  - regularity at $x \to -1$: g_{32}
  - regularity at $x \to -y/(1+y)$: $g_{41,44}$
  - regularity at $y \to 1$: $g_{16,23}$
  - regularity at $z \to 0$ and matching against their massless ($m_\ell = 0$) counterparts:

$$\begin{cases} h_a = \dfrac{g_1}{2} + g_4 + g_{25} - g_{37} - g_{38} + g_{45} \\ h_b = g_{30} \\ h_c = \dfrac{g_6}{4} + g_{21} \end{cases} \tag{3.27}$$

The boundary conditions for $h_{a,b,c}$ are determined from the $m_\ell \to 0$ behaviour of these integrals, where all the internal lepton propagators become massless. Around the $z = 0$ singularity, the differential equation for the z-evolution reduces to

$$\frac{\partial \mathbf{G}}{\partial z} \simeq \epsilon \, \frac{\mathbb{A}_{z,-1}}{z} \, \mathbf{G} \, . \tag{3.28}$$

To figure out the $m_\ell \to 0$ behaviour of the 46 MIs, we perform a Jordan decomposition of the pole matrix $\mathbb{A}_{z,-1}$ [92], i.e.,

$$\mathbb{A}_{z,-1} = \mathbb{S}^{-1} \mathbb{J} \, \mathbb{S} \, , \tag{3.29}$$

where $\mathbb{J}$ is the Jordan canonical form of $\mathbb{A}_{z,-1}$,

$$\mathbb{J} = \begin{pmatrix} -2 \times \mathbb{1}_{3\times 3} & & & \\ & \begin{pmatrix} -2 & 1 \\ 0 & -2 \end{pmatrix} & & \\ & & -1 \times \mathbb{1}_{9\times 9} & \\ & & & 0 \times \mathbb{1}_{32\times 32} \end{pmatrix} , \tag{3.30}$$

[3] The asymptotic behaviour of $\mathbf{G}$ in the limit $\alpha_i \to 0$ ($i = 1, \ldots, 7$) is provided in appendix C.

JHEP07(2022)078

and the similarity transformation $\mathbb{S}$ reads

$$\begin{pmatrix}
0 & 0 & 0 & 0 & 0 & 0 & 0 & 0 & \frac{1}{4} & 0 & -1 & \frac{1}{4} & 0 & 0 & 0 & 0 & -\frac{1}{2} & -\frac{1}{2} & 0 & 0 & 0 & 0 & 0 & 0 & 0 & 0 & 0 & 0 & 0 & 1 & \frac{1}{2} & -\frac{1}{2} & 0 & 0 & 0 & 0 & 0 & 0 & 0 & 0 & 0 & 0 & 0 & 0 \\
0 & 0 & 0 & 0 & 0 & 0 & \frac{1}{4} & 0 & 0 & -\frac{1}{4} & \frac{3}{2} & 1 & -\frac{1}{4} & 0 & 0 & 0 & 0 & \frac{1}{2} & \frac{1}{2} & 0 & 0 & 0 & 0 & 0 & 0 & 0 & 0 & 0 & 0 & 0 & -1 & -\frac{1}{2} & \frac{1}{2} & 0 & 0 & 0 & 0 & 0 & 0 & 0 & 0 & 0 & 0 & 0 & 0 \\
0 & 0 & 0 & 0 & 0 & 0 & 0 & 0 & 0 & 0 & -\frac{1}{2} & -\frac{1}{2} & 0 & 0 & 0 & 0 & 0 & -1 & 0 & 0 & 0 & 0 & 0 & 0 & 0 & 0 & 0 & 0 & 0 & 0 & 0 & 0 & 0 & 0 & 0 & 0 & 0 & 0 & 0 & 0 & 0 & 0 & 0 & 0 \\
\frac{1}{2} & 0 & 0 & 0 & 0 & 0 & \frac{1}{2} & 0 & 0 & 0 & 0 & -\frac{3}{2} & 0 & 0 & 0 & 0 & 0 & 0 & 0 & -1 & 0 & 0 & 0 & 0 & 0 & 0 & 0 & 0 & 0 & 0 & 0 & 0 & 0 & 0 & 0 & 0 & 0 & 0 & 0 & 0 & 0 & 0 & 0 & 0 \\
0 & 0 & 0 & 0 & 0 & 0 & \frac{1}{2} & 0 & 0 & 0 & 0 & 0 & 0 & 0 & 0 & 0 & 0 & 0 & 0 & 0 & 0 & 0 & 0 & 0 & 0 & 0 & 0 & 0 & 0 & 0 & 0 & 0 & 0 & 0 & 0 & 0 & 0 & 0 & 0 & 0 & 0 & 0 & 0 \\
\frac{1}{6} & 0 & -1 & -1 & \frac{9}{8} & \frac{7}{24} & -\frac{1}{2} & \frac{1}{8} & -\frac{1}{2} & 1 & 1 & -\frac{1}{2} & 0 & 1 & -3 & 0 & 1 & 2 & \frac{2}{3} & 0 & 0 & 0 & 0 & 0 & 0 & \frac{3}{2} & \frac{1}{4} & 0 & 0 & -2 & 0 & 1 & 1 & 0 & -\frac{1}{3} & -\frac{2}{3} & 0 & 0 & 0 & 0 & 1 & 0 & 1 & 0 & -1 & 1 \\
-\frac{1}{2} & 0 & -1 & -1 & \frac{3}{4} & \frac{1}{4} & -\frac{1}{2} & \frac{1}{4} & 0 & 0 & 0 & 0 & -\frac{3}{2} & 1 & -\frac{3}{2} & -\frac{1}{2} & 0 & 0 & 0 & -1 & 0 & 0 & 0 & -\frac{3}{2} & \frac{1}{2} & 0 & 0 & 0 & 0 & 0 & 0 & 0 & 0 & 0 & 0 & 0 & 0 & 0 & 0 & 0 & 0 & 0 & 0 & 0 & 0 & 0 \\
\frac{1}{3} & 0 & 1 & 1 & -\frac{3}{4} & -\frac{5}{12} & 0 & 0 & \frac{1}{2} & -\frac{5}{2} & -1 & \frac{1}{2} & \frac{3}{2} & -1 & 3 & 0 & -1 & -2 & -\frac{5}{3} & 0 & 0 & 0 & 0 & 0 & 0 & 0 & 0 & 0 & 0 & 2 & 0 & -1 & -1 & 0 & \frac{1}{3} & -\frac{1}{3} & 0 & 0 & 0 & 0 & -1 & 0 & -1 & 0 & 1 & -1 \\
0 & 0 & 0 & 0 & 0 & \frac{9}{8} & \frac{1}{8} & 0 & \frac{1}{8} & 0 & 0 & 0 & 0 & -\frac{3}{2} & 1 & -\frac{3}{2} & -\frac{1}{2} & 0 & 0 & 0 & -1 & 0 & 0 & 0 & -\frac{3}{2} & \frac{1}{2} & -\frac{3}{2} & -\frac{1}{4} & 0 & 0 & 0 & 0 & 0 & 0 & 0 & 0 & 0 & 0 & 0 & 0 & 0 & 0 & 0 & 0 & 0 & 0 \\
0 & 0 & 0 & 0 & 0 & \frac{3}{2} & -\frac{1}{2} & 0 & 0 & 0 & 0 & 0 & 0 & 0 & 1 & 0 & 0 & 0 & 0 & 0 & -1 & 0 & 0 & 0 & 0 & 0 & 0 & 0 & 0 & 0 & 0 & 0 & 0 & 0 & 0 & 0 & 0 & 0 & 0 & 0 & 0 & 0 & 0 & 0 & 0 \\
0 & 0 & 0 & 0 & 0 & -\frac{3}{4} & \frac{3}{4} & 0 & 0 & 0 & 0 & 0 & 0 & -\frac{3}{2} & 0 & 0 & 0 & 0 & 0 & 0 & 0 & 0 & 0 & 0 & 0 & 0 & 0 & 0 & 0 & 0 & 0 & 0 & 0 & 0 & 0 & 0 & 0 & 0 & 0 & 0 & 0 & 0 & 0 & 0 & 0 \\
-\frac{1}{2} & 0 & 0 & 0 & 0 & -\frac{1}{2} & 0 & 0 & 0 & 0 & \frac{3}{2} & 0 & 0 & 0 & 0 & 0 & 0 & 0 & 0 & 1 & 0 & 0 & 0 & 0 & 0 & 0 & 0 & 0 & 0 & 0 & 0 & 0 & 0 & 0 & 1 & 0 & 0 & 0 & 0 & 0 & 0 & 0 & 0 & 0 \\
1 & 0 & 0 & 0 & 0 & 0 & 0 & 0 & 0 & 0 & 0 & 0 & 0 & 0 & 0 & 0 & 0 & 0 & 0 & 0 & 0 & 0 & 0 & 0 & 0 & 0 & 0 & 0 & 0 & 0 & 0 & 0 & 0 & 0 & 0 & 0 & 0 & 0 & 0 & 0 & 0 & 0 & 0 \\
0 & 0 & 0 & 0 & -\frac{1}{8} & -\frac{1}{8} & -\frac{1}{6} & -\frac{5}{24} & 0 & 0 & 0 & 0 & \frac{1}{2} & 0 & 0 & 0 & 0 & 0 & 0 & 0 & 0 & 0 & 0 & 0 & 0 & 0 & \frac{3}{2} & \frac{1}{4} & 0 & 0 & 0 & 0 & 0 & 0 & 0 & 0 & 0 & 0 & 0 & 0 & 0 & 0 & 0 & 0 & 0 & 0 \\
-\frac{1}{6} & 0 & 1 & 1 & -\frac{9}{8} & -\frac{7}{24} & \frac{1}{2} & -\frac{1}{8} & \frac{1}{4} & -1 & 0 & \frac{1}{4} & 0 & -1 & 3 & 0 & -\frac{1}{2} & -\frac{3}{2} & -\frac{2}{3} & 0 & 0 & 0 & 0 & 0 & 0 & -\frac{3}{2} & -\frac{1}{4} & 0 & 0 & 1 & -\frac{1}{2} & -\frac{1}{2} & -1 & 0 & \frac{1}{3} & \frac{2}{3} & 0 & 0 & 0 & 0 & -1 & 0 & -1 & 0 & 1 & 0 \\
\frac{1}{2} & 0 & 1 & 1 & -\frac{3}{4} & -\frac{1}{4} & \frac{1}{2} & -\frac{1}{4} & 0 & 0 & 0 & 0 & \frac{3}{2} & -1 & \frac{3}{2} & \frac{1}{2} & 0 & 0 & 0 & 1 & 0 & 0 & 0 & \frac{3}{2} & -\frac{1}{2} & 0 & 0 & 0 & 0 & 0 & 0 & 0 & 0 & 0 & 0 & 0 & 0 & 0 & 0 & 0 & 0 & 0 & 0 & 0 & 1 & 0 \\
-\frac{1}{3} & 0 & -1 & -1 & \frac{3}{4} & \frac{1}{6} & 0 & 0 & -\frac{1}{4} & 1 & 0 & -\frac{1}{4} & -\frac{3}{2} & 1 & -3 & 0 & \frac{1}{2} & \frac{3}{2} & \frac{5}{3} & 0 & 0 & 0 & 0 & 0 & 0 & 0 & 0 & 0 & -1 & \frac{1}{2} & \frac{1}{2} & 1 & 0 & -\frac{1}{3} & \frac{1}{3} & 0 & 0 & 0 & 0 & 1 & 0 & 1 & 1 & -1 & 1 \\
0 & 0 & 0 & 0 & 0 & 0 & 0 & 0 & 0 & 0 & 0 & 0 & 0 & 0 & 0 & 0 & 0 & 0 & 0 & 0 & 0 & 0 & 0 & 0 & 0 & 0 & 0 & 0 & 0 & 0 & 0 & 0 & 0 & 0 & 0 & 0 & 0 & 0 & 0 & 0 & 1 & 0 & 0 & 0 \\
0 & 0 & 0 & 0 & 0 & 0 & 0 & 0 & 0 & 0 & 0 & 0 & 0 & 0 & 0 & 0 & 0 & 0 & 0 & 0 & 0 & 0 & 0 & 0 & 0 & 0 & 0 & 0 & 0 & 0 & 0 & 0 & 0 & 0 & 0 & 0 & 0 & 0 & 0 & 0 & 0 & 1 & 0 & 0 \\
0 & 0 & 0 & 0 & -\frac{9}{8} & -\frac{1}{8} & 0 & -\frac{1}{8} & 0 & 0 & 0 & 0 & \frac{3}{2} & -1 & \frac{3}{2} & \frac{1}{2} & 0 & 0 & 0 & 1 & 0 & 0 & 0 & \frac{3}{2} & -\frac{1}{2} & \frac{3}{2} & \frac{1}{4} & 0 & 0 & 0 & 0 & 0 & 0 & 0 & 0 & 0 & 0 & 0 & 0 & 0 & 0 & 0 & 0 & 1 & 0 & 0 & 0 \\
0 & 0 & 0 & 0 & 0 & 0 & 0 & 0 & \frac{1}{2} & \frac{1}{2} & 0 & 0 & 0 & 0 & 0 & 1 & 0 & 0 & 0 & 0 & 0 & 0 & 0 & 0 & 0 & 0 & 0 & 0 & 0 & 0 & 0 & 0 & 0 & 0 & 0 & 0 & 0 & 0 & 0 & 0 & 0 & 1 & 0 & 0 & 0 \\
0 & 0 & 0 & 0 & 0 & 0 & 0 & 0 & 0 & 0 & 0 & 0 & 0 & 0 & 0 & 0 & 0 & 0 & 0 & 0 & 0 & 0 & 0 & 0 & 0 & 0 & 0 & 0 & 0 & 0 & 0 & 0 & 0 & 0 & 0 & 0 & 0 & 0 & 0 & 0 & 0 & 0 & 1 & 0 & 0 & 0 \\
0 & 0 & 0 & 0 & -\frac{3}{2} & \frac{1}{4} & 0 & 0 & 0 & 0 & 0 & 0 & -1 & 0 & 0 & 0 & 0 & 0 & 1 & 0 & 0 & 0 & 0 & 0 & 0 & 0 & 0 & 0 & 0 & 0 & 0 & 0 & 0 & 0 & 0 & 0 & 1 & 0 & 0 & 0 & 0 & 0 & 0 & 0 & 0 \\
0 & 0 & 0 & 0 & \frac{3}{4} & -\frac{1}{2} & 0 & 0 & 0 & 0 & 0 & 0 & \frac{3}{2} & 0 & 0 & 0 & 0 & 0 & 0 & 0 & 0 & 0 & 0 & 0 & 0 & 0 & 0 & 0 & 0 & 0 & 0 & 0 & 0 & 0 & 0 & 0 & 0 & 1 & 0 & 0 & 0 & 0 & 0 & 0 & 0 \\
-\frac{1}{2} & 0 & 0 & 0 & 0 & -\frac{1}{2} & 0 & 0 & 0 & 0 & 0 & 0 & 0 & 0 & 0 & 0 & 0 & 0 & 1 & 0 & 0 & 0 & 0 & 0 & 0 & 0 & 0 & 0 & 0 & 0 & 0 & 0 & 0 & 1 & 2 & 0 & 0 & 0 & 0 & 0 & 0 & 0 & 0 & 0 \\
0 & 0 & 0 & 0 & 0 & 0 & 0 & 0 & 0 & 1 & 1 & 0 & 0 & 0 & 0 & 0 & 2 & 0 & 0 & 0 & 0 & 0 & 0 & 0 & 0 & 0 & 0 & 0 & 0 & 0 & 0 & 0 & 0 & 1 & 0 & 0 & 0 & 0 & 0 & 0 & 0 & 0 & 0 & 0 \\
0 & 0 & 0 & 0 & 0 & 0 & 0 & 0 & 0 & 0 & 0 & 0 & 0 & 0 & 0 & 0 & 0 & 0 & 0 & 0 & 0 & 0 & 0 & 0 & 0 & 0 & 0 & 0 & 0 & 0 & 0 & 0 & 0 & 0 & 1 & 0 & 0 & 0 & 0 & 0 & 0 & 0 & 0 & 0 \\
-\frac{1}{2} & 0 & 0 & 0 & 0 & 0 & 0 & 0 & 0 & \frac{1}{4} & -1 & -\frac{1}{2} & \frac{1}{4} & 0 & 0 & 0 & 0 & \frac{1}{2} & -\frac{1}{2} & -1 & 0 & 0 & 0 & 0 & 0 & 0 & 0 & 0 & 0 & 0 & 1 & \frac{1}{2} & \frac{1}{2} & 0 & 0 & 0 & 0 & 0 & 0 & 0 & 0 & 0 & 0 & 0 & 0 \\
0 & 0 & 0 & 0 & 0 & 0 & 0 & 0 & 0 & -\frac{1}{4} & 0 & 1 & -\frac{1}{4} & 0 & 0 & 0 & 0 & \frac{1}{2} & \frac{1}{2} & 0 & 0 & 0 & 0 & 0 & 0 & 0 & 0 & 0 & 0 & -1 & \frac{1}{2} & \frac{1}{2} & 0 & 0 & 0 & 0 & 0 & 0 & 0 & 0 & 0 & 0 & 0 & 0 \\
0 & 0 & 0 & 0 & 0 & 0 & 0 & 0 & 0 & 0 & 0 & 0 & 0 & 0 & 0 & 0 & 0 & 0 & 0 & 0 & 0 & 0 & 0 & 0 & 0 & 0 & 0 & 0 & 0 & 1 & 0 & 0 & 0 & 0 & 0 & 0 & 0 & 0 & 0 & 0 & 0 & 0 & 0 & 0 \\
0 & 0 & 0 & 0 & 0 & 0 & 0 & 0 & 0 & 0 & 0 & 0 & 0 & 0 & 0 & 0 & 0 & 0 & 0 & 0 & 0 & 0 & 0 & 0 & 0 & 0 & 0 & 0 & 0 & 0 & 1 & 0 & 0 & 0 & 0 & 0 & 0 & 0 & 0 & 0 & 0 & 0 & 0 & 0 \\
0 & 0 & 0 & 0 & 0 & 0 & 0 & 0 & 0 & 0 & 0 & 0 & 0 & 0 & 0 & 0 & 0 & 0 & 0 & 0 & 0 & 0 & 0 & 0 & 0 & 0 & 0 & 0 & 0 & 0 & 0 & 1 & 0 & 0 & 0 & 0 & 0 & 0 & 0 & 0 & 0 & 0 & 0 & 0 \\
0 & 0 & 0 & 0 & \frac{3}{4} & -\frac{3}{4} & -1 & \frac{1}{4} & 0 & 0 & 0 & 0 & 3 & 0 & 0 & 0 & 0 & 0 & 0 & 0 & 0 & 0 & 0 & 0 & 0 & 3 & \frac{3}{2} & 0 & 0 & 0 & 0 & 0 & 0 & 0 & 0 & 0 & 0 & 0 & 0 & 0 & 0 & 0 & 0 & 0 & 0 \\
0 & 0 & 0 & 0 & \frac{1}{8} & \frac{1}{8} & \frac{1}{6} & \frac{5}{24} & 0 & 0 & 0 & 0 & -\frac{1}{2} & 0 & 0 & 0 & 0 & 0 & 0 & 0 & 0 & 0 & 0 & 0 & 0 & -\frac{1}{2} & -\frac{1}{4} & 0 & 0 & 0 & 0 & 0 & 0 & 0 & 0 & 0 & 0 & 0 & 0 & 0 & 0 & 0 & 0 & 0 & 0 \\
0 & 0 & 0 & 0 & 0 & 0 & -\frac{1}{2} & \frac{1}{4} & 0 & 0 & 0 & 0 & 0 & 0 & -\frac{3}{2} & -\frac{1}{2} & 0 & 0 & 0 & 0 & 0 & 0 & 0 & -\frac{3}{2} & \frac{3}{2} & 0 & 0 & 0 & 0 & 0 & 0 & 0 & 0 & 0 & 0 & 0 & 0 & 0 & 0 & 0 & 0 & 0 & 0 & 0 & 0 \\
0 & 0 & 0 & 0 & 0 & 0 & -\frac{1}{6} & -\frac{1}{12} & 0 & 0 & 0 & 0 & 0 & 0 & -\frac{3}{2} & -\frac{1}{2} & 0 & 0 & 0 & 0 & 0 & 0 & 0 & -\frac{1}{2} & \frac{1}{2} & 0 & 0 & 0 & 0 & 0 & 0 & 0 & 0 & 0 & 0 & 0 & 0 & 0 & 0 & 0 & 0 & 0 & 0 & 0 & 0 \\
0 & 0 & 0 & 0 & 0 & -\frac{1}{4} & 0 & 0 & 0 & 0 & 0 & 0 & 0 & 0 & 0 & 0 & 0 & 0 & 0 & 1 & 0 & 0 & 0 & 0 & 0 & 0 & 0 & 0 & 0 & 0 & 0 & 0 & 0 & 0 & 0 & 0 & 0 & 0 & 0 & 0 & 0 & 0 & 0 & 0 \\
0 & 0 & 0 & 0 & 0 & 0 & 0 & 0 & 0 & -\frac{1}{2} & 0 & 0 & 0 & 0 & 0 & 0 & 0 & 0 & 0 & 0 & 1 & 0 & 0 & 0 & 0 & 0 & 0 & 0 & 0 & 0 & 0 & 0 & 0 & 0 & 0 & 0 & 0 & 0 & 0 & 0 & 0 & 0 & 0 & 0 \\
0 & 0 & 0 & 0 & 0 & \frac{1}{4} & 0 & 0 & 0 & 0 & 0 & 0 & 0 & 0 & 0 & 0 & 0 & 0 & 0 & 0 & 0 & 1 & 0 & 0 & 0 & 0 & 0 & 0 & 0 & 0 & 0 & 0 & 0 & 0 & 0 & 0 & 0 & 0 & 0 & 0 & 0 & 0 & 0 & 0 \\
0 & 0 & 0 & 0 & \frac{3}{2} & 0 & 0 & 0 & 0 & 0 & 0 & 0 & 1 & 0 & 0 & 0 & 0 & 0 & 0 & 0 & 0 & 0 & 1 & 0 & 0 & 0 & 0 & 0 & 0 & 0 & 0 & 0 & 0 & 0 & 0 & 0 & 0 & 0 & 0 & 0 & 0 & 0 & 0 & 0 \\
\frac{1}{2} & 0 & 0 & 0 & 0 & 0 & 0 & 0 & 0 & 1 & 0 & 0 & 0 & 0 & 0 & 0 & 1 & 1 & 0 & 0 & 0 & 0 & 0 & 0 & 0 & 0 & 0 & 0 & 0 & 0 & 0 & 0 & 0 & 0 & 0 & 0 & 0 & 0 & 0 & 0 & 0 & 0 & 0 & 0 \\
0 & 0 & 0 & 0 & 0 & 0 & 0 & 0 & 0 & 0 & -\frac{1}{2} & 0 & 0 & 0 & 0 & 0 & 0 & 0 & 0 & 0 & 0 & 0 & 0 & 0 & 0 & 0 & 0 & 0 & 0 & 0 & 0 & 0 & 0 & 0 & 0 & 0 & 0 & 0 & 0 & 0 & 0 & 0 & 0 & 0 \\
0 & 0 & 0 & 0 & 0 & 0 & 0 & 0 & 0 & 0 & 0 & 0 & 0 & 0 & 0 & 1 & 0 & 0 & 0 & 0 & 0 & 0 & 0 & 0 & 0 & 0 & 0 & 0 & 0 & 0 & 0 & 0 & 0 & 0 & 0 & 0 & 0 & 0 & 0 & 0 & 0 & 0 & 0 & 0 \\
0 & 0 & 0 & 0 & 0 & 0 & 0 & 0 & -1 & 0 & 0 & 0 & 0 & 0 & 1 & 0 & 0 & 0 & 0 & 0 & 0 & 0 & 0 & 0 & 0 & 0 & 0 & 0 & 0 & 0 & 0 & 0 & 0 & 0 & 0 & 0 & 0 & 0 & 0 & 0 & 0 & 0 & 0 & 0 \\
0 & 0 & -1 & 0 & 0 & 0 & 0 & 0 & 0 & 0 & 0 & 0 & 0 & 0 & 0 & 0 & 0 & 0 & 0 & 0 & 0 & 0 & 0 & 0 & 0 & 0 & 0 & 0 & 0 & 0 & 0 & 0 & 0 & 0 & 0 & 0 & 0 & 0 & 0 & 0 & 0 & 0 & 0 & 0 \\
0 & 1 & 0 & 0 & 0 & 0 & 0 & 0 & 0 & 0 & 0 & 0 & 0 & 0 & 0 & 0 & 0 & 0 & 0 & 0 & 0 & 0 & 0 & 0 & 0 & 0 & 0 & 0 & 0 & 0 & 0 & 0 & 0 & 0 & 0 & 0 & 0 & 0 & 0 & 0 & 0 & 0 & 0 & 0
\end{pmatrix} \tag{3.31}$$

Then the z-evolution around the $z = 0$ singularity can be described in Jordan form,

$$\frac{\partial \mathbf{H}}{\partial z} \simeq \epsilon \, \frac{\mathbb{J}}{z} \, \mathbf{H} \,, \tag{3.32}$$

where $\mathbf{H} = (h_1, h_2, \ldots, h_{46})^T$ is the Jordan canonical basis defined by $\mathbf{H} = \mathbb{S}\,\mathbf{G}$. Considering the Jordan block structure of $\mathbb{J}$, the singular behaviour of $\mathbf{H}$ in the limit $z \to 0$ can be simply factored out, and the solution of eq. (3.32) can be expressed as

$$\mathbf{H} = \mathbb{R}^{-1}\mathbf{H}_0 \,, \qquad \mathbb{R} = z^{2\epsilon}\, \mathbb{1}_{3\times 3} \oplus z^{2\epsilon} \begin{pmatrix} 1 & -\epsilon \log z \\ 0 & 1 \end{pmatrix} \oplus z^{\epsilon}\, \mathbb{1}_{9\times 9} \oplus \mathbb{1}_{32\times 32} \,, \tag{3.33}$$

where $\mathbf{H}_0 = (h_{1,0}, h_{2,0}, \ldots, h_{46,0})^T$ is analytic at $z = 0$. For convenience, we define

$$\widetilde{\mathbf{H}} = (h_1, h_2, \ldots, h_{14})^T \,, \qquad \widehat{\mathbf{H}} = (h_{15}, h_{16}, \ldots, h_{46})^T \,, \tag{3.34}$$

JHEP07(2022)078

and

$$\widetilde{\mathbb{R}} = z^{2\epsilon}\,\mathbb{1}_{3\times3} \oplus z^{2\epsilon} \begin{pmatrix} 1 & -\epsilon\log z \\ 0 & 1 \end{pmatrix} \oplus z^{\epsilon}\,\mathbb{1}_{9\times9}\,. \tag{3.35}$$

The regularity of $\mathbb{R}\mathbf{H}$ at $z \to 0$ can be applied to the following two aspects.

1. *Boundary conditions:*

$$\lim_{z\to0} \widehat{\mathbf{H}} = \mathbb{K}\,\mathbf{I}\,. \tag{3.36}$$

$\widehat{\mathbf{H}}$ is analytic at $z = 0$, the l.h.s. of eq. (3.36) can be computed by taking the limit $z \to 0$ directly at the integrand level and thus expressed in terms of the canonical basis $\mathbf{I} = (\mathrm{I}_1, \mathrm{I}_2, \ldots, \mathrm{I}_{31})^T$ of the two-loop scalar integrals involved in the mixed QCD-QED virtual corrections to the charged-current Drell-Yan production of a massless charged lepton [65].

In eq. (3.27) we introduced three two-loop scalar integrals h_a, h_b and h_c for fixing the boundary terms of $\mathbf{G}$. Considering the analytic expression of $\mathbb{S}$ in eq. (3.31), $h_{a,b,c}$ can be written as linear combinations of $\widehat{\mathbf{H}}$,

$$\begin{aligned} h_a &= h_{16} - h_{23} - h_{24} + h_{35} + h_{45}\,, \\ h_b &= h_{30}\,, \\ h_c &= h_{39}\,, \end{aligned} \tag{3.37}$$

and thus are finite in the limit $z \to 0$. After performing IBP reduction, we obtain

$$\begin{aligned} \lim_{z\to0}\, h_a &= -\,\mathrm{I}_{11} - \mathrm{I}_{17} + \mathrm{I}_{23} - \mathrm{I}_{26} + \mathrm{I}_{29} + \mathrm{I}_{31}\,, \\ \lim_{z\to0}\, h_b &= \mathrm{I}_{13}\,, \\ \lim_{z\to0}\, h_c &= \mathrm{I}_{8}\,. \end{aligned} \tag{3.38}$$

The matching of $h_{a,b,c}$ to their massless counterparts, i.e., eq. (3.38), provides three boundary conditions for $\mathbf{G}$.

2. *Consistency checks:*

$$\widetilde{\mathbb{R}}\,\widetilde{\mathbf{H}}\text{: finite in the limit } z \to 0 \tag{3.39}$$

Even though $z = 0$ is a singularity of $\widetilde{\mathbf{H}}$, $\widetilde{\mathbb{R}}\widetilde{\mathbf{H}}$ is finite when $z \to 0$. Thus, the finiteness of the following 14 combinations of $\widetilde{\mathbf{H}}$ in the zero lepton mass limit provides a consistency check for the analytic solution of the canonical differential system (3.9),

$$\begin{aligned} &z^{2\epsilon}\,h_{1,2,3,5}\,, \\ &z^{\epsilon}\,h_{6,7,8,9,10,11,12,13,14}\,, \\ &z^{2\epsilon}\,(h_4 - \epsilon\log z\,h_5)\,. \end{aligned} \tag{3.40}$$

3.4 Solution and checks

We obtain the solution of the canonical differential system (3.9) in terms of GPLs of arguments x, y and z with weights $\{0, -1, -y, -y/(1+y)\}$, $\{0, 1\}$ and $\{0\}$, respectively. The analytic expressions of all the 46 canonical MIs up to $\mathcal{O}(\epsilon^4)$ in the second-order approximation (i.e., eq. (3.18)) are provided in electronic form via supplementary material attached to this paper. Since the weight of GPLs with argument z is zero, the lepton-mass singularities of $\mathbf{G}$ must be the logarithms of the form $\log^n(m_\ell^2/m_W^2)$ which can be completely determined by the leading terms in the z-expansion of $\mathbb{A}_{x,y,z}$. In appendix D, we showcase the explicit expressions of g_i $(i = 1, \ldots, 46)$ up to $\mathcal{O}(\epsilon^3)$ in the lowest-order approximation, i.e., setting $\{\mathbb{A}_x, \mathbb{A}_y, \mathbb{A}_z\} = \{\mathbb{A}_{x,0}, \mathbb{A}_{y,0}, \mathbb{A}_{z,-1}/z\}$. In order to verify our analytic solution we performed a number of checks:

- We checked our results in the Euclidean region $\{(x, y, z) \,|\, x > 0,\, 0 < y < 1,\, z > 0\}$ against the numerical values obtained with `pySecDec` [93, 94] based on the sector decomposition algorithm. A comparison between the numerical results obtained from our analytic expressions and `pySecDec` for some representative MIs at $s = -5$, $t = -2$, $m_\ell^2 = 10^{-3}$ and $m_W^2 = 4\,\text{GeV}^2$ is presented in table 1. It shows that all these numerical results are in good agreement with each other within the calculation errors.

- The canonical basis $\mathbf{\Gamma} = (\gamma_1, \gamma_2, \ldots, \gamma_7)^T$ for the integral set $\mathcal{S}_{\text{aux}}$ defined by eq. (B.4) was calculated analytically in appendix B. As a corollary of eq. (B.10), the MIs g_1, g_5, g_6, g_{10}, g_{13}, g_{18}, g_{19}, as functions of x and z, must satisfy the following identities:

$$g_{1,5,6,10,13,18,19}(x = 1, z) = \gamma_{1,2,4,3,7,5,6}(z)\,. \tag{3.41}$$

  These identities were verified at the analytical level in the lowest-order approximation up to $\mathcal{O}(\epsilon^4)$.[4]

- The $m_\ell \to 0$ behaviour of the Jordan canonical basis $\mathbf{H} = \mathbb{S}\,\mathbf{G}$ was checked.

  - As stated in section 3.3, h_i $(i = 15, \ldots, 46)$ are finite in the limit $z \to 0$, and their massless counterparts can be expressed as the linear combinations of I_1, I_2, …, and I_{31}. The correctness of eq. (3.36) was confirmed by employing IBP recurrence relations and, consequently, the explicit expression of the 32×31 matrix $\mathbb{K}$ was obtained.

  - h_i $(i = 1, \ldots, 14)$ are divergent as $m_\ell \to 0$, but the 14 combinations of them defined by eq. (3.40) are finite in the zero lepton mass limit. The asymptotic behaviour of these combinations in the limit $z \to 0$ was checked both analytically and numerically, which clearly demonstrate the regularity of these combinations at $z = 0$.

[4] The analytic expressions for γ_i $(i = 1, \ldots, 7)$ in the lowest-order approximation can be obtained from eq. (B.9) by setting the GPLs with non-zero weight to zero.

JHEP07(2022)078

$$\mathbb{K} = \begin{pmatrix}
-\frac{15}{8} & \frac{1}{8} & \frac{7}{16} & \frac{1}{2} & 0 & \frac{1}{16} & -\frac{3}{2} & 0 & 3 & -1 & 0 & \frac{1}{4} & 0 & -\frac{1}{2} & 0 & \frac{1}{2} & 0 & -\frac{1}{2} & 0 & \frac{3}{4} & -\frac{1}{8} & 0 & 0 & 0 & 0 & 0 & \frac{1}{2} & -\frac{1}{2} & 0 & 0 & 1 \\
0 & 0 & 0 & 0 & 0 & 0 & 0 & 0 & 0 & 0 & 0 & 0 & 0 & 0 & 0 & 0 & 0 & 0 & 0 & 0 & 0 & 0 & 0 & 0 & 0 & 0 & 0 & 1 & 0 & 1 \\
0 & 0 & 0 & 0 & 0 & 0 & 0 & 0 & 0 & 0 & 0 & 0 & 0 & 0 & 0 & 0 & 0 & 0 & 0 & 0 & 0 & 0 & 0 & 0 & 0 & 0 & 0 & 0 & 1 & 0 \\
\frac{7}{8} & \frac{7}{8} & -\frac{7}{16} & -\frac{1}{2} & 0 & -\frac{1}{16} & \frac{1}{2} & 0 & 0 & 0 & 0 & -\frac{1}{4} & 0 & -\frac{1}{2} & 0 & -\frac{1}{6} & 0 & \frac{1}{2} & 0 & -\frac{7}{4} & \frac{1}{8} & 0 & 0 & 0 & 0 & 0 & -\frac{1}{2} & \frac{1}{2} & 0 & 0 & 0 \\
0 & 0 & 0 & 0 & 0 & 0 & 0 & 0 & 0 & 0 & 0 & 0 & 0 & 0 & 0 & 0 & 0 & 0 & 0 & 0 & 0 & 0 & 0 & 0 & 0 & 1 & 0 & 0 & 0 & 0 \\
0 & 0 & 0 & 0 & 0 & 0 & 0 & 0 & 0 & 0 & 0 & 0 & 0 & 0 & 0 & 0 & 0 & 0 & 0 & 0 & 0 & 0 & 0 & 0 & 0 & 0 & 0 & 1 & 0 & 0 \\
0 & 0 & 0 & 0 & 0 & 0 & 0 & 0 & 0 & 0 & 0 & 0 & 0 & 0 & 0 & 0 & 0 & 0 & 0 & 0 & 0 & 0 & 0 & 0 & 1 & 0 & 0 & 0 & 0 & 0 \\
0 & 0 & 0 & 0 & 0 & 0 & 0 & 0 & 0 & 0 & 0 & 0 & 0 & 0 & 0 & 0 & 0 & 0 & 0 & 0 & 0 & 0 & 0 & 1 & 0 & 0 & 0 & 0 & 0 & 0 \\
0 & 0 & 0 & 0 & 0 & 0 & 0 & 0 & 0 & 0 & 0 & 0 & 0 & 0 & 0 & 0 & 0 & 0 & 0 & 0 & 0 & 0 & 1 & 0 & 0 & 0 & 0 & 0 & 0 & 0 \\
0 & 0 & 0 & 0 & 0 & 0 & 0 & 0 & 0 & 0 & 0 & 0 & 0 & 0 & 0 & 0 & 0 & 0 & 0 & 0 & 0 & 1 & 0 & 0 & 0 & 0 & 0 & 0 & 0 & 0 \\
0 & 0 & 0 & 0 & 0 & 0 & 0 & 0 & 0 & 0 & 0 & 0 & 0 & 0 & 0 & 0 & 1 & 0 & 0 & 0 & 0 & 0 & 0 & 0 & 0 & 0 & 0 & 0 & 0 & 0 \\
0 & 0 & 0 & 0 & 0 & 0 & 0 & 0 & 0 & 0 & 0 & 0 & 0 & 0 & 0 & 1 & 0 & 0 & 0 & 0 & 0 & 0 & 0 & 0 & 0 & 0 & 0 & 0 & 0 & 0 \\
0 & 0 & 0 & 0 & 0 & 0 & 0 & 0 & 0 & 0 & 0 & 0 & 0 & 0 & 0 & 0 & 0 & 0 & 0 & 0 & 1 & 0 & 0 & 0 & 0 & 0 & 0 & 0 & 0 & 0 \\
0 & 0 & 0 & 0 & 0 & 0 & 0 & 0 & 0 & 0 & 0 & 0 & 0 & 0 & 0 & 0 & 0 & 0 & 0 & 1 & 0 & 0 & 0 & 0 & 0 & 0 & 0 & 0 & 0 & 0 \\
-1 & -\frac{3}{2} & \frac{1}{2} & 0 & 0 & 0 & -1 & 0 & 0 & 0 & 0 & 0 & 2 & 1 & 0 & 0 & 0 & 0 & 0 & 0 & 0 & 0 & 0 & 0 & 0 & 0 & 0 & 0 & 0 & 0 \\
0 & 0 & 0 & 0 & 0 & 0 & 0 & 0 & 0 & 0 & 0 & 0 & 0 & 1 & 0 & 0 & 0 & 0 & 0 & 0 & 0 & 0 & 0 & 0 & 0 & 0 & 0 & 0 & 0 & 0 \\
0 & 0 & 0 & 0 & 0 & 0 & 0 & 0 & 0 & 0 & 0 & 0 & 1 & 0 & 0 & 0 & 0 & 0 & 0 & 0 & 0 & 0 & 0 & 0 & 0 & 0 & 0 & 0 & 0 & 0 \\
0 & 0 & 0 & 0 & 0 & 0 & 0 & 0 & 0 & 0 & 0 & 0 & 0 & 0 & 0 & 0 & 0 & 1 & 0 & 0 & 0 & 0 & 0 & 0 & 0 & 0 & 0 & 0 & 0 & 0 \\
0 & 0 & 0 & 0 & 0 & 0 & 0 & 0 & 0 & 0 & 0 & 0 & 0 & 1 & 0 & 0 & 0 & 0 & 0 & 0 & 0 & 0 & 0 & 0 & 0 & 0 & 0 & 0 & 0 & 0 \\
0 & 0 & 0 & 0 & \frac{3}{2} & \frac{3}{2} & 0 & 0 & 0 & 0 & 0 & 0 & 0 & 0 & 0 & 0 & 0 & 0 & 0 & 0 & -6 & 0 & 0 & 0 & 0 & 0 & 0 & 0 & 0 & 0 \\
0 & 0 & 0 & 0 & 0 & 0 & 0 & 0 & 0 & 0 & 0 & 0 & 0 & 0 & 0 & 0 & 0 & 0 & 0 & 0 & 1 & 0 & 0 & 0 & 0 & 0 & 0 & 0 & 0 & 0 \\
0 & 0 & 0 & 0 & 0 & 0 & 0 & 0 & 0 & 0 & 0 & 0 & 0 & 0 & 0 & 0 & 0 & 0 & 0 & 0 & 0 & 1 & 0 & 0 & 0 & 0 & 0 & 0 & 0 & 0 \\
0 & 0 & 0 & 0 & 0 & -\frac{1}{6} & 0 & 0 & -1 & 0 & 0 & -\frac{1}{3} & 0 & 0 & 0 & 0 & 0 & 0 & 0 & 0 & 0 & 0 & \frac{1}{3} & 0 & 0 & 0 & 0 & 0 & 0 & 0 \\
0 & 0 & 0 & 0 & 0 & 0 & 0 & 0 & 0 & 0 & 0 & 0 & 0 & 0 & 0 & 0 & 0 & 0 & 1 & 0 & 0 & 0 & 0 & 0 & 0 & 0 & 0 & 0 & 0 & 0 \\
0 & 0 & 0 & 0 & 0 & 0 & 0 & 1 & 0 & 0 & 0 & 0 & 0 & 0 & 0 & 0 & 0 & 0 & 0 & 0 & 0 & 0 & 0 & 0 & 0 & 0 & 0 & 0 & 0 & 0 \\
0 & 0 & 0 & 0 & 0 & 0 & 0 & 1 & 0 & 0 & 0 & 0 & 0 & 0 & 0 & 0 & 0 & 0 & 0 & 0 & 0 & 0 & 0 & 0 & 0 & 0 & 0 & 0 & 0 & 0 \\
1 & 0 & 0 & 0 & 0 & 0 & 0 & 0 & 0 & 1 & 0 & 0 & 0 & 0 & 0 & 0 & 0 & 0 & 0 & 0 & 0 & 0 & 0 & 0 & 0 & 0 & 0 & 0 & 0 & 0 \\
0 & 0 & 0 & 0 & 0 & 0 & 1 & 0 & 0 & 0 & 0 & 0 & 0 & 0 & 0 & 0 & 0 & 0 & 0 & 0 & 0 & 0 & 0 & 0 & 0 & 0 & 0 & 0 & 0 & 0 \\
0 & -\frac{1}{2} & 0 & 0 & 0 & 0 & 0 & 0 & 0 & 0 & 0 & 0 & 0 & 0 & 0 & 0 & 0 & 0 & 0 & 0 & 0 & 0 & 0 & 0 & 0 & 0 & 0 & 0 & 0 & 0 \\
0 & 0 & 0 & 0 & 0 & 0 & 0 & 0 & 0 & 0 & 0 & 1 & 0 & 0 & 0 & 0 & 0 & 0 & 0 & 0 & 0 & 0 & 0 & 0 & 0 & 0 & 0 & 0 & 0 & 0 \\
2 & 0 & 0 & 0 & 0 & 0 & 0 & 0 & 1 & 0 & 0 & 0 & 0 & 0 & 0 & 0 & 0 & 0 & 0 & 0 & 0 & 0 & 0 & 0 & 0 & 0 & 0 & 0 & 0 & 0 \\
0 & 0 & 0 & 0 & 0 & 0 & 0 & 0 & 0 & -1 & 0 & 0 & 0 & 0 & 0 & 0 & 0 & 0 & 0 & 0 & 0 & 0 & 0 & 0 & 0 & 0 & 0 & 0 & 0 & 0 \\
0 & 0 & 0 & 1 & 0 & 0 & 0 & 0 & 0 & 0 & 0 & 0 & 0 & 0 & 0 & 0 & 0 & 0 & 0 & 0 & 0 & 0 & 0 & 0 & 0 & 0 & 0 & 0 & 0 & 0
\end{pmatrix} \tag{3.42}$$

4 Summary

The DY production of dilepton via Z and single lepton via W in hadron-hadron collisions is one of the cutting-edge topics in the field of high energy physics. In this paper we present an analytic calculation of the MIs for the mixed QCD-QED two-loop virtual corrections to the charged-current DY process $q\bar{q}' \to \ell\nu$. The scalar Feynman integrals involved in the non-factorizable corrections can be expressed in terms of the linear combinations of 46 MIs, which satisfy a set of first-order differential equations. By means of a suitable basis transformation, we obtain a canonical set of MIs. The ϵ-dependence of the canonical differential system is factorized from the kinematics. Therefore, the canonical MIs, as the solution of the canonical differential system, can be cast in a Taylor series around $d = 4$, with coefficients written in terms of Chen's iterated integrals. After an expansion for small z, all the entries of the coefficient matrices are simple rational functions, and thus the Chen's iterated integrals can be expressed in terms of GPLs. The boundary constants of these canonical MIs are fixed by using known or simpler integrals as independent input and by requiring the regularity of the solution at some special kinematic limits. We solve the canonical differential system in the second-order approximation and then obtain the Taylor series expansions of the 46 canonical MIs around $d = 4$ up to $\mathcal{O}(\epsilon^4)$, which contain all the logarithmic terms of the form $z^m \log^n z$ ($m = 0, 1,\ n = 0, 1, 2, 3, 4$). As for the factorizable corrections, the related MIs are either included in the 46 MIs for the non-

JHEP07(2022)078

G	*Analytic* $[\mathcal{O}(z\log^n z)]$ / *Analytic* $[\mathcal{O}(z^2\log^n z)]$ / `pySecDec`
g_{13}	$41.2060921304982\,\epsilon^2 + 363.015345460615\,\epsilon^3 + 1991.43341346475\,\epsilon^4$
	$41.2060921304982\,\epsilon^2 + 363.015343632027\,\epsilon^3 + 1991.43340188216\,\epsilon^4$
	$41.20609213041(25)\,\epsilon^2 + 363.01537(5)\,\epsilon^3 + 1991.4338(8)\,\epsilon^4$
g_{26}	$47.5646588551249\,\epsilon^3 + 359.901210192870\,\epsilon^4$
	$47.5646586479934\,\epsilon^3 + 359.901217045946\,\epsilon^4$
	$47.564661(5)\,\epsilon^3 + 359.901218(29)\,\epsilon^4$
g_{41}	$-41.1936546266871\,\epsilon^3 - 312.411476285700\,\epsilon^4$
	$-41.1936549977326\,\epsilon^3 - 312.411485581619\,\epsilon^4$
	$-41.193654989(13)\,\epsilon^3 - 312.41134(22)\,\epsilon^4$
g_{46}	$7.71826798162703\,\epsilon^2 + 22.3660080321417\,\epsilon^3 - 81.8728881227263\,\epsilon^4$
	$7.71826825644108\,\epsilon^2 + 22.3660072472345\,\epsilon^3 - 81.8729064820082\,\epsilon^4$
	$7.718268257(1)\,\epsilon^2 + 22.3647(16)\,\epsilon^3 - 81.885(12)\,\epsilon^4$

Table 1. Comparison between the numerical results obtained from our analytic expressions and `pySecDec` for g_{13}, g_{26}, g_{41} and g_{46} at $(s,\, t,\, m_\ell^2,\, m_W^2) = (-5, -2,\, 10^{-3},\, 4)$ GeV^2.

factorizable corrections or obtained from the literature. Our analytic results can help to implement a flexible and efficient MC program for precision analysis of charged-current DY processes when the finite-lepton-mass effect is taken into consideration.

Acknowledgments

This work is supported in part by the National Natural Science Foundation of China (Grants No. 11775211 and No. 12061141005) and the CAS Center for Excellence in Particle Physics (CCEPP).

A Mixed QCD-QED virtual corrections to $q\bar{q}' \to W^*$

The 20 two-loop Feynman diagrams for the mixed QCD-QED virtual corrections to $q\bar{q}' \to W^*$ can be categorized into 8 topologies belonging to 3 vertex integral families $\mathcal{F}_{1,2,3}$. Some representative topologies of these Feynman diagrams are depicted in figure 3.

- *Family* $\mathcal{F}_1$:

$$\begin{aligned} &D_1 = l_1^2\,, && D_2 = (l_1+p_1)^2\,, && D_3 = (l_1-p_2)^2\,,\\ &D_4 = l_2^2\,, && D_5 = (l_2+p_1)^2\,, && D_6 = (l_2-p_2)^2\,, \\ &D_7 = (l_1-l_2)^2 \end{aligned} \tag{A.1}$$

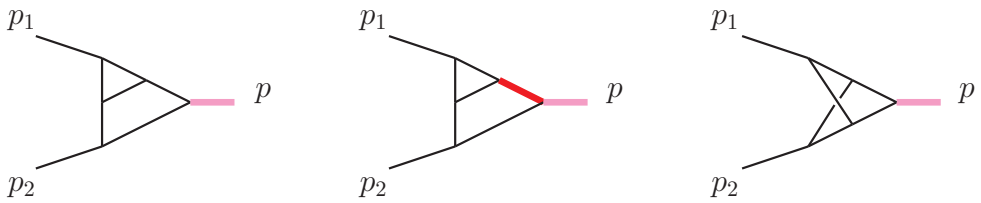

Figure 3. Three representative topologies of Feynman diagrams belonging to $\mathcal{F}_1$, $\mathcal{F}_2$ and $\mathcal{F}_3$ respectively for mixed QCD-QED two-loop virtual corrections to $q\bar{q}' \to W^*$.

3 *topologies* $\subset \mathcal{F}_1$:

$$[1,1,1,1,1,0,1]\,, \qquad [1,1,1,0,1,1,1]\,, \qquad [1,1,1,0,1,0,1] \tag{A.2}$$

It is worth mentioning that $[1,1,1,0,1,0,1]$ is the sub-sector of $[1,1,1,1,1,0,1]$ and $[1,1,1,0,1,1,1]$. The two-loop scalar integrals belonging to $\mathcal{S}_1$,

$$\mathcal{S}_1 \equiv [1,1,1,1,1,0,1]_F \cup [1,1,1,0,1,1,1]_F\,, \tag{A.3}$$

can be reduced to 3 MIs f_5, f_a and f_b, where f_a and f_b are depicted schematically in figure 4.

- *Family* $\mathcal{F}_2$:

$$\begin{aligned} &D_1 = l_1^2\,, && D_2 = (l_1+p_1)^2 - m_W^2\,, && D_3 = (l_1-p_2)^2\,, \\ &D_4 = l_2^2\,, && D_5 = (l_2+p_1)^2\,, && D_6 = (l_2-p_2)^2\,, \\ &D_7 = (l_1-l_2)^2 \end{aligned} \tag{A.4}$$

4 *topologies* $\subset \mathcal{F}_2$:

$$[1,1,1,1,1,0,1]\,, \qquad [1,1,1,1,0,1,1]\,, \qquad [0,1,1,1,1,1,1]\,, \qquad [1,1,1,1,0,0,1] \tag{A.5}$$

In eq. (A.5) the last sector is the sub-sector of the first two sectors. All the two-loop scalar integrals of $\mathcal{F}_2$ involved in the mixed QCD-QED virtual corrections to $q\bar{q}' \to W^*$ belong to $\mathcal{S}_2$,

$$\mathcal{S}_2 \equiv [1,1,1,1,1,0,1]_F \cup [1,1,1,1,0,1,1]_F \cup [0,1,1,1,1,1,1]_F\,. \tag{A.6}$$

The 9 MIs of this integral set can be chosen as $f_2, f_3, f_5, f_9, f_{11}, f_{12}, f_{14}, f_{15}, f_{28}$.

- *Family* $\mathcal{F}_3$:

$$\begin{aligned} &D_1 = l_1^2\,, && D_2 = (l_1+p_1)^2\,, && D_3 = (l_1-p_2)^2\,, \\ &D_4 = (l_2+p_1)^2\,, && D_5 = (l_2-p_2)^2\,, && D_6 = (l_1-l_2)^2\,, \\ &D_7 = (l_1-l_2+p_2)^2 \end{aligned} \tag{A.7}$$

1 *topology* $\subset \mathcal{F}_3$:

$$[1,1,0,1,1,1,1] \tag{A.8}$$

JHEP07(2022)078

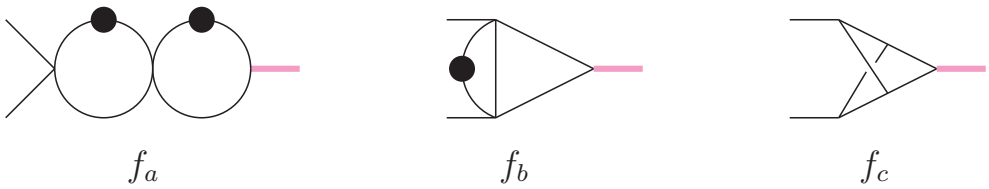

Figure 4. Three MIs for mixed QCD-QED two-loop virtual corrections to $q\bar{q}' \to W^*$.

Unlike the 7 topologies in eqs. (A.2) and (A.5), $[1,1,0,1,1,1,1]$ in eq. (A.8) is a three-point non-planar topology, which is represented schematically by the non-planar graph in figure 3. The two-loop scalar integrals induced by the non-planar Feynman diagrams via tensor reduction belong to $\mathcal{S}_3$,

$$\mathcal{S}_3 \equiv [1,1,0,1,1,1,1]_F\,, \tag{A.9}$$

and can be reduced to a set of 3 MIs f_5, f_b and f_c, where f_c is a non-planar two-loop scalar integral defined by the last graph in figure 4.

In summary, there are totally 12 MIs for the mixed QCD-QED two-loop virtual corrections to $q\bar{q}' \to W^*$, which can be chosen as

$$g_2,\ g_3,\ g_5,\ g_9,\ g_{11},\ g_{12},\ g_{14},\ g_{15},\ g_{28},\ f_a,\ f_b,\ f_c\,. \tag{A.10}$$

All the two-loop scalar integrals involved in the calculation of mixed QCD-QED virtual corrections to $q\bar{q}' \to W^*$ contain at most two energy scales, the invariant mass $\sqrt{s}$ and the W-boson mass m_W. Being the same as f_i and g_i $(i = 1,\ldots,46)$, $f_{a,b,c}$ have been nondimensionalized by the W-boson mass; thus the 12 MIs in eq. (A.10) should depend only on the dimensionless variable $x = -s/m_W^2$.[5] The first 9 MIs, $g_{2,3,5,9,11,12,14,15,28}$, have been included in the 46 MIs for the non-factorizable mixed QCD-QED two-loop virtual corrections to $q\bar{q}' \to \ell\nu$. For the remaining 3 MIs, $f_{a,b,c}$ (depicted in figure 4), their analytic expressions in terms of GPLs up to weight 4 can be obtained from the literature [65, 95].

B Auxiliary integrals

In this appendix we discuss the computation of the auxiliary vertex integrals used to extract the boundary constants of g_{13} and g_{18} in section 3.3. The two-loop vertex integral family considered here is identified by the set of propagators

$$\begin{aligned}
&D_1 = l_1^2\,, && D_2 = l_2^2\,, && D_3 = (l_1 - l_2)^2\,,\\
&D_4 = (l_1 + p_1)^2 - m_\ell^2\,, && D_5 = (l_2 + p_1 + p_2)^2\,, && D_6 = (l_2 + p_1)^2\,,\\
&D_7 = (l_1 + p_1 + p_2)^2\,,
\end{aligned} \tag{B.1}$$

[5] From figure 2 and eq. (3.8), we may conclude that $g_{2,3,5,9,11,12,14,15,28}$ are only functions of x, while the other 37 components of $\mathbf{G}$ depend also on y and/or z.

JHEP07(2022)078

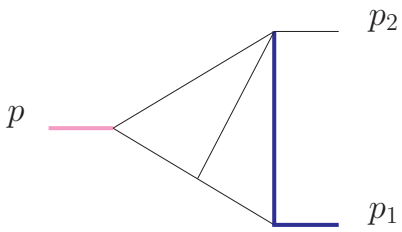

Figure 5. Sector $[1,1,1,1,1,0,0]$ of the vertex integral family identified by eq. (B.1).

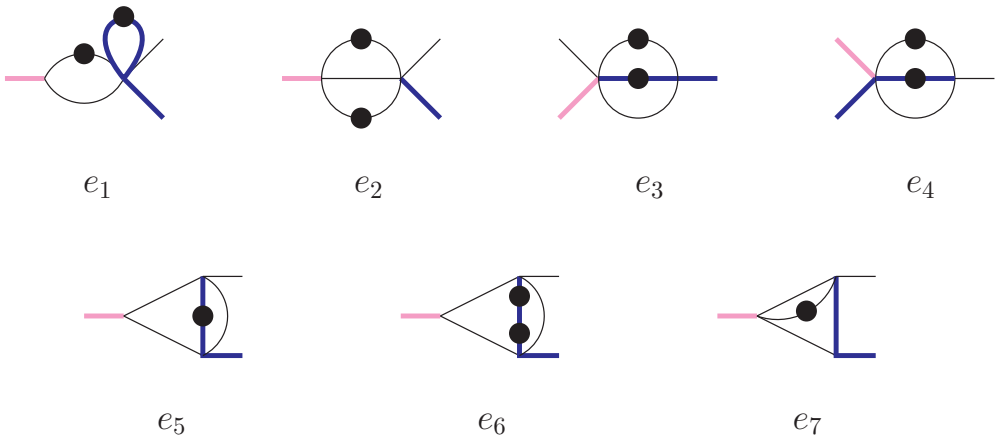

Figure 6. A set of pre-canonical MIs for $\mathcal{S}_{\text{aux}}$.

with external momenta p_1, p_2 and p satisfying

$$p_1^2 = m_\ell^2\,, \qquad p_2^2 = 0\,, \qquad (p_1+p_2)^2 = p^2 = s\,. \tag{B.2}$$

Now we focus on the sector $[1,1,1,1,1,0,0]$ (depicted in figure 5) of this integral family. It is obvious that

$$\begin{aligned} f_{13} &\in [1,0,1,1,1,0,0] \\ f_{18} &\in [0,1,1,1,1,0,0] \end{aligned} \subset [1,1,1,1,1,0,0]_F\,. \tag{B.3}$$

All the integrals belonging to $\mathcal{S}_{\text{aux}} \equiv [1,1,1,1,1,0,0]_F$ have the form of

$$\int \mathcal{D}^d l_1 \mathcal{D}^d l_2 \frac{D_6^{n_6} D_7^{n_7}}{D_1^{n_1} D_2^{n_2} D_3^{n_3} D_4^{n_4} D_5^{n_5}}\,, \qquad (n_{1,\ldots,5} \in \mathbb{Z}, \quad n_{6,7} \in \mathbb{N})\,, \tag{B.4}$$

and can be reduced to a set of 7 MIs shown in figure 6. These MIs ($e_i,\ i = 1,\ldots,7$) have been nondimensionalized by $(-s)$, and thus can be expressed as functions of the dimensionless variable κ,

$$\kappa = -\frac{m_\ell^2}{s}\,. \tag{B.5}$$

JHEP07(2022)078

The canonical basis $\mathbf{\Gamma} = (\gamma_1, \gamma_2, \ldots, \gamma_7)^T$, defined by eq. (B.6),

$$\begin{aligned}
&\gamma_1 = \epsilon^2\, e_1\,, && \gamma_2 = \epsilon^2\, e_2\,,\\
&\gamma_3 = \epsilon^2\, e_3\, \kappa\,, && \gamma_4 = \epsilon\,(1-\epsilon)\, e_4\, \kappa\,,\\
&\gamma_5 = \epsilon^3\, e_5\,(1+\kappa)\,, && \gamma_6 = \epsilon^2\, e_6\, \kappa\,(1+\kappa)\,,\\
&\gamma_7 = \epsilon^3\, e_7\,(1+\kappa)\,,
\end{aligned} \tag{B.6}$$

satisfies the following $d\log$-form total differential equation,

$$d\mathbf{\Gamma} = \epsilon\left[\mathbb{M}_1\, d\log(\kappa) + \mathbb{M}_2\, d\log(\kappa+1)\right]\mathbf{\Gamma}\,, \tag{B.7}$$

where

$$\mathbb{M}_1 = \begin{pmatrix}
-1 & 0 & 0 & 0 & 0 & 0 & 0\\
0 & 0 & 0 & 0 & 0 & 0 & 0\\
0 & 0 & -2 & 0 & 0 & 0 & 0\\
0 & 0 & 0 & -2 & 0 & 0 & 0\\
0 & 0 & 2 & \frac{1}{2} & 0 & 2 & 0\\
\frac{1}{2} & 0 & 0 & -\frac{1}{2} & 0 & -2 & 0\\
0 & -\frac{1}{2} & 0 & -\frac{1}{2} & 0 & 0 & -1
\end{pmatrix}, \qquad \mathbb{M}_2 = \begin{pmatrix}
0 & 0 & 0 & 0 & 0 & 0 & 0\\
0 & 0 & 0 & 0 & 0 & 0 & 0\\
0 & 0 & 0 & 0 & 0 & 0 & 0\\
0 & 0 & 0 & 0 & 0 & 0 & 0\\
0 & 0 & 0 & 0 & -1 & -2 & 0\\
0 & 0 & 0 & 0 & 3 & 4 & 0\\
0 & 0 & 0 & 0 & 0 & 0 & 2
\end{pmatrix}. \tag{B.8}$$

The same strategy as in section 3.2 is applied here to solve the canonical differential system in eq. (B.7). To determine the unknown integration constants, the four simple integrals $\gamma_{1,2,3,4}$ serve as input to this system [65, 74]. As for $\gamma_{5,6,7}$, the integration constants are fixed by the regularity at $\kappa \to -1$. Then we obtain the solution of the canonical differential system (B.7) in terms of GPLs of argument κ,[6]

$$\begin{aligned}
\gamma_1 =\;& 1 - \epsilon\, G(0;\kappa) + \epsilon^2\big[G(0,0;\kappa) + \zeta(2)\big] - \epsilon^3\big[\zeta(2)\, G(0;\kappa) + G(0,0,0;\kappa) - 2\,\zeta(3)\big]\\
&- \epsilon^4/4\big[8\,\zeta(3)\, G(0;\kappa) - 4\,\zeta(2)\, G(0,0;\kappa) - 4\, G(0,0,0,0;\kappa) - 19\,\zeta(4)\big] + \mathcal{O}(\epsilon^5)\,,\\
\gamma_2 =\;& -1 + 6\,\epsilon^3\,\zeta(3) + 9\,\epsilon^4\,\zeta(4) + \mathcal{O}(\epsilon^5)\,,\\
\gamma_3 =\;& -1/4 + \epsilon/2\, G(0;\kappa) - \epsilon^2/2\big[2\, G(0,0;\kappa) + 3\,\zeta(2)\big] + \epsilon^3\big[3\,\zeta(2)\, G(0;\kappa) + 2\, G(0,0,0;\kappa) - 3\,\zeta(3)\big]\\
&+ 2\,\epsilon^4\big[3\,\zeta(3)\, G(0;\kappa) - 3\,\zeta(2)\, G(0,0;\kappa) - 2\, G(0,0,0,0;\kappa) - 12\,\zeta(4)\big] + \mathcal{O}(\epsilon^5)\,,\\
\gamma_4 =\;& 1 - 2\,\epsilon\, G(0;\kappa) + 4\,\epsilon^2\big[G(0,0;\kappa) + \zeta(2)\big] - 2\,\epsilon^3\big[4\,\zeta(2)\, G(0;\kappa) + 4\, G(0,0,0;\kappa) - \zeta(3)\big]\\
&- \epsilon^4\big[4\,\zeta(3)\, G(0;\kappa) - 16\,\zeta(2)\, G(0,0;\kappa) - 16\, G(0,0,0,0;\kappa) - 31\,\zeta(4)\big] + \mathcal{O}(\epsilon^5)\,,\\
\gamma_5 =\;& \epsilon^3\big[2\,\zeta(2)\, G(0;\kappa) - 3\,\zeta(2)\, G(-1;\kappa) + G(0,0,0;\kappa) - G(-1,0,0;\kappa) - \zeta(3)\big]\\
&- \epsilon^4\big[\zeta(3)\, G(0;\kappa) + 3\,\zeta(3)\, G(-1;\kappa) + 7\,\zeta(2)\, G(0,0;\kappa) - 7\,\zeta(2)\, G(-1,0;\kappa)\\
&- 12\,\zeta(2)\, G(0,-1;\kappa) + 9\,\zeta(2)\, G(-1,-1;\kappa) + 5\, G(0,0,0,0;\kappa) - 4\, G(-1,0,0,0;\kappa)\\
&- 4\, G(0,-1,0,0;\kappa) + 3\, G(-1,-1,0,0;\kappa) + 14\,\zeta(4)\big] + \mathcal{O}(\epsilon^5)\,,\\
\gamma_6 =\;& \epsilon^2/2\big[G(0,0;\kappa) + 3\,\zeta(2)\big] - \epsilon^3/2\big[9\,\zeta(2)\, G(0;\kappa) - 12\,\zeta(2)\, G(-1;\kappa) + 5\, G(0,0,0;\kappa)\\
&- 4\, G(-1,0,0;\kappa) - 4\,\zeta(3)\big] - \epsilon^4/8\big[32\,\zeta(3)\, G(0;\kappa) - 40\,\zeta(3)\, G(-1;\kappa) - 100\,\zeta(2)\, G(0,0;\kappa)\\
&+ 96\,\zeta(2)\, G(-1,0;\kappa) + 96\,\zeta(2)\, G(0,-1;\kappa) - 120\,\zeta(2)\, G(-1,-1;\kappa) - 68\, G(0,0,0,0;\kappa)\\
&+ 56\, G(-1,0,0,0;\kappa) + 32\, G(0,-1,0,0;\kappa) - 40\, G(-1,-1,0,0;\kappa) - 285\,\zeta(4)\big] + \mathcal{O}(\epsilon^5)\,,
\end{aligned}$$

[6] We have also calculated $\mathbf{\Gamma}$ by using the `Maple` program `HyperInt` [96], and obtained the same results as in eq. (B.9).

JHEP07(2022)078

$$\begin{aligned}\gamma_7 = \epsilon^2\big[G(0,0;\kappa)+3\,\zeta(2)\big] - \epsilon^3\big[5\,\zeta(2)\,G(0;\kappa) - 6\,\zeta(2)\,G(-1;\kappa) + 3\,G(0,0,0;\kappa) - 2\,G(-1,0,0;\kappa)\\ - 2\,\zeta(3)\big] - \epsilon^4/4\big[24\,\zeta(3)\,G(0;\kappa) - 16\,\zeta(3)\,G(-1;\kappa) - 36\,\zeta(2)\,G(0,0;\kappa) + 40\,\zeta(2)\,G(-1,0;\kappa)\\ + 24\,\zeta(2)\,G(0,-1;\kappa) - 48\,\zeta(2)\,G(-1,-1;\kappa) - 28\,G(0,0,0,0;\kappa) + 24\,G(-1,0,0,0;\kappa)\\ + 8\,G(0,-1,0,0;\kappa) - 16\,G(-1,-1,0,0;\kappa) - 89\,\zeta(4)\big] + \mathcal{O}(\epsilon^5)\,. \end{aligned} \tag{B.9}$$

By the definition of $\mathbf{G}$ and $\mathbf{\Gamma}$ we can see that

$$(g_1,\, g_5,\, g_{10},\, g_6,\, g_{18},\, g_{19},\, g_{13})^T = x^{-2\epsilon}\,\mathbf{\Gamma} \quad \text{with} \quad \kappa = z/x\,. \tag{B.10}$$

Thus, the boundary constants of g_{13} and g_{18} are given by the constant components of γ_7 and γ_5, respectively,

$$\begin{aligned} c_{13} &= \gamma_{7,\text{const}} = 3\,\zeta(2)\,\epsilon^2 + 2\,\zeta(3)\,\epsilon^3 + \frac{89}{4}\,\zeta(4)\,\epsilon^4 + \mathcal{O}(\epsilon^5)\,,\\ c_{18} &= \gamma_{5,\text{const}} = -\zeta(3)\,\epsilon^3 - 14\,\zeta(4)\,\epsilon^4 + \mathcal{O}(\epsilon^5)\,. \end{aligned} \tag{B.11}$$

C Asymptotic behaviour of G

We analyze the asymptotic behaviour of $\mathbf{G}$ in the limit $\alpha_i \to 0$ $(i = 1, \ldots, 7)$ by using the code `asy.m` [97, 98] included in `FIESTA` [99, 100] and summarize it in table 2.

g_i	$s \to 0$	$s \to -t$	$s \to m_W^2$	$t \to 0$	$m_\ell^2 \to 0$	$t \to -m_W^2$	$s \to \frac{m_W^2 t}{t - m_W^2}$
1	×	✓	✓	✓	×	✓	✓
2	×	✓	✓	✓	✓	✓	✓
3	✓	✓	×	✓	✓	✓	✓
4	✓	✓	×	✓	×	✓	✓
5	×	✓	✓	✓	✓	✓	✓
6	✓	✓	✓	✓	×	✓	✓
7	✓	✓	✓	×	×	✓	✓
8	✓	✓	✓	×	✓	✓	✓
9	✓	✓	✓	✓	✓	✓	✓
10	✓	✓	✓	✓	×	✓	✓
11	✓	✓	×	✓	✓	✓	✓
12	✓	✓	×	✓	✓	✓	✓
13	×	✓	✓	✓	×	✓	✓
14	×	✓	×	✓	✓	✓	✓
15	✓	✓	×	✓	✓	✓	✓
16	✓	✓	✓	✓	✓	✓	✓
17	✓	✓	×	✓	×	✓	✓

Table 2. The kinematic limits $s \to 0$, $s \to m_W^2$, $s \to -t$, $s \to m_W^2 t/(t - m_W^2)$, $t \to 0$, $t \to -m_W^2$ and $m_\ell^2 \to 0$ correspond to $\alpha_i \to 0$, $i = 1, \ldots, 7$, respectively. The chechmark means the MI is analytic, while the cross singular, in the corresponding limit (continues).

JHEP07(2022)078

g_i	$s\to 0$	$s\to -t$	$s\to m_W^2$	$t\to 0$	$m_\ell^2\to 0$	$t\to -m_W^2$	$s\to \dfrac{m_W^2 t}{t-m_W^2}$
18	×	✓	✓	✓	×	✓	✓
19	×	✓	✓	✓	×	✓	✓
20	×	✓	×	✓	×	✓	✓
21	✓	✓	✓	×	×	✓	✓
22	✓	✓	✓	×	×	✓	✓
23	✓	✓	✓	×	×	✓	✓
24	✓	✓	×	×	×	✓	✓
25	✓	✓	×	×	×	✓	✓
26	×	✓	✓	×	×	✓	✓
27	×	✓	✓	×	×	✓	✓
28	✓	✓	✓	✓	✓	✓	✓
29	✓	✓	✓	✓	✓	✓	✓
30	✓	✓	✓	✓	✓	✓	✓
31	✓	✓	×	✓	×	✓	✓
32	×	✓	✓	✓	×	✓	✓
33	✓	✓	✓	×	✓	✓	✓
34	✓	✓	×	×	×	✓	✓
35	×	✓	✓	×	×	✓	✓
36	×	✓	✓	×	×	✓	✓
37	×	✓	✓	×	×	✓	✓
38	×	✓	×	×	×	✓	✓
39	✓	✓	✓	✓	✓	✓	✓
40	✓	✓	×	×	×	✓	✓
41	×	✓	×	×	×	✓	✓
42	×	✓	✓	✓	✓	✓	✓
43	×	✓	×	×	×	✓	✓
44	×	✓	×	×	×	✓	✓
45	×	✓	×	×	×	✓	✓
46	✓	✓	×	×	×	✓	✓

Table 2. The kinematic limits $s\to 0$, $s\to m_W^2$, $s\to -t$, $s\to m_W^2 t/(t-m_W^2)$, $t\to 0$, $t\to -m_W^2$ and $m_\ell^2\to 0$ correspond to $\alpha_i\to 0,\ i=1,\ldots,7$, respectively. The chechmark means the MI is analytic, while the cross singular, in the corresponding limit.

D Explicit expressions of G

The analytic expressions of the 46 canonical MIs g_i $(i=1,\ldots,46)$ in terms of GPLs up to $\mathcal{O}(\epsilon^3)$ in the lowest-order approximation are listed as follows:

$$g_1 = 1-\epsilon\big[G(0;x)+G(0;z)\big]+\epsilon^2\big[G(0;x)G(0;z)+G(0,0;x)+G(0,0;z)+\zeta(2)\big]-\epsilon^3\big[\zeta(2)G(0;x)$$
$$+\zeta(2)G(0;z)+G(0;x)G(0,0;z)+G(0;z)G(0,0;x)+G(0,0,0;x)+G(0,0,0;z)-2\zeta(3)\big],$$

$$
\begin{aligned}
g_2 &= 1-\epsilon G(0;x)+\epsilon^2\big[G(0,0;x)+\zeta(2)\big]-\epsilon^3\big[\zeta(2)\,G(0;x)+G(0,0,0;x)-2\zeta(3)\big]\,,\\
g_3 &= -\epsilon G(-1;x)+\epsilon^2\big[G(-1,0;x)+2G(-1,-1;x)\big]-\epsilon^3\big[\zeta(2)\,G(-1;x)+G(-1,0,0;x)\\
&\quad +2G(-1,-1,0;x)+4G(-1,-1,-1;x)\big]\,,\\
g_4 &= \epsilon^2\big[G(-1;x)\,G(0;z)-G(0,-1;x)\big]-\epsilon^3\big[G(-1;x)\,G(0,0;z)+G(0;z)\,G(-1,0;x)\\
&\quad -G(0;z)\,G(0,-1;x)+2G(0;z)\,G(-1,-1;x)-G(0,-1,0;x)+G(0,0,-1;x)\\
&\quad -2G(-1,0,-1;x)-2G(0,-1,-1;x)\big]\,,\\
g_5 &= -1+2\epsilon G(0;x)-4\epsilon^2 G(0,0;x)+\epsilon^3\big[8G(0,0,0;x)+6\zeta(3)\big]\,,\\
g_6 &= 1-2\epsilon G(0;z)+4\epsilon^2\big[G(0,0;z)+\zeta(2)\big]-2\epsilon^3\big[4\zeta(2)\,G(0;z)+4G(0,0,0;z)-\zeta(3)\big]\,,\\
g_7 &= \epsilon\big[G(0;y)-G(0;z)\big]+\epsilon^2\big[G(0;y)\,G(0;z)-3G(0,0;y)+G(0,0;z)+\zeta(2)\big]-\epsilon^3\big[\zeta(2)\,G(0;y)\\
&\quad +\zeta(2)\,G(0;z)+G(0;y)\,G(0,0;z)+G(0;z)\,G(0,0;y)-7G(0,0,0;y)+G(0,0,0;z)-8\zeta(3)\big]\,,\\
g_8 &= -1+2\epsilon G(0;y)-4\epsilon^2 G(0,0;y)+\epsilon^3\big[8G(0,0,0;y)+6\zeta(3)\big]\,,\\
g_9 &= 1+4\zeta(2)\,\epsilon^2+2\zeta(3)\,\epsilon^3\,,\\
g_{10} &= -1/4+\epsilon/2\,G(0;z)-\epsilon^2/2\big[2G(0,0;z)+3\zeta(2)\big]+\epsilon^3\big[3\zeta(2)\,G(0;z)+2G(0,0,0;z)-3\zeta(3)\big]\,,\\
g_{11} &= \epsilon G(-1;x)+\epsilon^2\big[G(0,-1;x)-4G(-1,-1;x)\big]+\epsilon^3\big[4\zeta(2)\,G(-1;x)+G(0,0,-1;x)\\
&\quad -6G(-1,0,-1;x)-4G(0,-1,-1;x)+16G(-1,-1,-1;x)\big]\,,\\
g_{12} &= -1+2\epsilon G(-1;x)+4\epsilon^2\big[G(0,-1;x)-2G(-1,-1;x)-\zeta(2)\big]+2\epsilon^3\big[4\zeta(2)\,G(-1;x)\\
&\quad +2G(0,0,-1;x)-6G(-1,0,-1;x)-8G(0,-1,-1;x)+16G(-1,-1,-1;x)-\zeta(3)\big]\,,\\
g_{13} &= -\epsilon^2\big[G(0;x)\,G(0;z)-G(0,0;x)-G(0,0;z)-3\zeta(2)\big]-\epsilon^3\big[\zeta(2)\,G(0;x)+5\zeta(2)\,G(0;z)\\
&\quad -G(0;x)\,G(0,0;z)-G(0;z)\,G(0,0;x)+3G(0,0,0;x)+3G(0,0,0;z)-2\zeta(3)\big]\,,\\
g_{14} &= 1-\epsilon\big[2G(0;x)+G(-1;x)\big]+\epsilon^2\big[4G(0,0;x)+G(-1,0;x)-G(0,-1;x)+2G(-1,-1;x)\big]\\
&\quad -\epsilon^3\big[2\zeta(2)\,G(-1;x)+8G(0,0,0;x)+2G(-1,0,0;x)-G(0,-1,0;x)+G(0,0,-1;x)\\
&\quad +2G(-1,-1,0;x)-2G(-1,0,-1;x)-2G(0,-1,-1;x)+4G(-1,-1,-1;x)+6\zeta(3)\big]\,,\\
g_{15} &= -\epsilon/2\,G(-1;x)-\epsilon^2/2\big[G(0,-1;x)-3G(-1,-1;x)\big]-\epsilon^3/2\big[4\zeta(2)\,G(-1;x)\\
&\quad +G(0,0,-1;x)-3G(-1,0,-1;x)-3G(0,-1,-1;x)+9G(-1,-1,-1;x)\big]\,,\\
g_{16} &= \epsilon^2 G(1,0;y)+\epsilon^3\big[2\zeta(2)\,G(1;y)-2G(1,0,0;y)+G(0,1,0;y)-2G(1,1,0;y)\big]\,,\\
g_{17} &= -\epsilon^2\big[G(-1;x)\,G(0;z)-G(0,-1;x)\big]+\epsilon^3\big[\zeta(2)\,G(-1;x)+2G(-1;x)\,G(0,0;z)\\
&\quad -3G(0;z)\,G(0,-1;x)+4G(0;z)\,G(-1,-1;x)+4G(0,0,-1;x)-3G(-1,0,-1;x)\\
&\quad -4G(0,-1,-1;x)\big]\,,\\
g_{18} &= -\epsilon^3\big[2\zeta(2)\,G(0;x)-2\zeta(2)\,G(0;z)+G(0;x)\,G(0,0;z)-G(0;z)\,G(0,0;x)+G(0,0,0;x)\\
&\quad -G(0,0,0;z)+\zeta(3)\big]\,,\\
g_{19} &= -\epsilon^2/2\big[G(0;x)\,G(0;z)-G(0,0;x)-G(0,0;z)-3\zeta(2)\big]+\epsilon^3/2\big[3\zeta(2)\,G(0;x)-9\zeta(2)\,G(0;z)\\
&\quad +3G(0;x)\,G(0,0;z)-G(0;z)\,G(0,0;x)-G(0,0,0;x)-5G(0,0,0;z)+4\zeta(3)\big]\,,
\end{aligned}
$$

JHEP07(2022)078

$$
\begin{aligned}
g_{20} = {} & \epsilon^2\big[G(0;x)\,G(0;z) - G(-1;x)\,G(0;z) - G(0,0;x) + G(0,-1;x) - G(0,0;z) - 3\zeta(2)\big] \\
& + \epsilon^3\big[\zeta(2)\,G(0;x) - 3\zeta(2)\,G(-1;x) + 5\zeta(2)\,G(0;z) - G(0;x)\,G(0,0;z) + G(-1;x)\,G(0,0;z) \\
& - G(0;z)\,G(0,0;x) + G(0;z)\,G(-1,0;x) - 2G(0;z)\,G(0,-1;x) + 2G(0;z)\,G(-1,-1;x) \\
& + 3G(0,0,0;x) - G(-1,0,0;x) - G(0,-1,0;x) + 3G(0,0,-1;x) - 2G(-1,0,-1;x) \\
& - 2G(0,-1,-1;x) + 3G(0,0,0;z) - 2\zeta(3)\big]\,,
\end{aligned}
$$

$$
\begin{aligned}
g_{21} = {} & -\epsilon/2\big[G(0;y) - G(0;z)\big] + \epsilon^2/2\big[2G(0,0;y) - 2G(0,0;z) - \zeta(2)\big] - \epsilon^3/2\big[2\zeta(2)\,G(0;y) \\
& - 4\zeta(2)\,G(0;z) + 4G(0,0,0;y) - 4G(0,0,0;z) + 3\zeta(3)\big]\,,
\end{aligned}
$$

$$
\begin{aligned}
g_{22} = {} & 1/8 - \epsilon/4\big[2G(0;y) - G(0;z)\big] + \epsilon^2/4\big[4G(0,0;y) - 2G(0,0;z) - \zeta(2)\big] - \epsilon^3/2\big[2\zeta(2)\,G(0;y) \\
& - 3\zeta(2)\,G(0;z) + 4G(0,0,0;y) - 2G(0,0,0;z) + 5\zeta(3)\big]\,,
\end{aligned}
$$

$$
\begin{aligned}
g_{23} = {} & \epsilon/2\big[G(0;y) - G(0;z)\big] - \epsilon^2/2\big[2G(0,0;y) - 2G(1,0;y) - 2G(0,0;z) - \zeta(2)\big] \\
& + \epsilon^3/2\big[2\zeta(2)\,G(0;y) + 2\zeta(2)\,G(1;y) - 4\zeta(2)\,G(0;z) + 4G(0,0,0;y) + 2G(0,1,0;y) \\
& - 4G(1,0,0;y) - 2G(1,1,0;y) - 4G(0,0,0;z) + 3\zeta(3)\big]\,,
\end{aligned}
$$

$$
\begin{aligned}
g_{24} = {} & \epsilon^2\big[G(-1;x)\,G(0;z) - G(0,-1;x)\big] + \epsilon^3\big[\zeta(2)\,G(-1;x) - G(-1;x)\,G(0;y)\,G(0;z) \\
& + G(-1;x)\,G(0,0;y) - G(-1;x)\,G(1,0;y) - G(-1;x)\,G(0,0;z) - G(0;y)\,G(-y,-1;x) \\
& + G(0;y)\,G(0,-1;x) + 3G(0;z)\,G(0,-1;x) - 3G(0;z)\,G(-1,-1;x) + G(-y;x)\,G(1,0;y) \\
& - 5G(0,0,-1;x) + 3G(-1,0,-1;x) + 3G(0,-1,-1;x) + G(-y,0,-1;x)\big]\,,
\end{aligned}
$$

$$
\begin{aligned}
g_{25} = {} & -1/6 + \epsilon/6\big[3G(-1;x) + 4G(0;y) - 2G(0;z)\big] + \epsilon^2/6\big[2G(0;y)\,G(0;z) + 6G(-1;x)\,G(0;z) \\
& - 12G(-1;x)\,G(0;y) + 9G(0,-1;x) - 9G(-1,-1;x) - 10G(0,0;y) + 6G(1,0;y) \\
& + 2G(0,0;z) + 2\zeta(2)\big] + \epsilon^3/6\big[-6\zeta(2)\,G(-1;x) - 2\zeta(2)\,G(0;y) + 12\zeta(2)\,G(1;y) \\
& - 2\zeta(2)\,G(0;z) - 6G(-1;x)\,G(0;y)\,G(0;z) + 30G(-1;x)\,G(0,0;y) - 18G(-1;x)\,G(1,0;y) \\
& - 6G(-1;x)\,G(0,0;z) + 18G(-y;x)\,G(1,0;y) - 2G(0;y)\,G(0,0;z) - 18G(0;y)\,G(0,-1;x) \\
& + 36G(0;y)\,G(-1,-1;x) - 18G(0;y)\,G(-y,-1;x) - 2G(0;z)\,G(0,0;y) \\
& + 18G(0;z)\,G(0,-1;x) - 18G(0;z)\,G(-1,-1;x) + 9G(0,0,-1;x) - 27G(-1,0,-1;x) \\
& - 27G(0,-1,-1;x) + 27G(-1,-1,-1;x) + 18G(-y,0,-1;x) + 22G(0,0,0;y) \\
& - 12G(1,0,0;y) + 6G(0,1,0;y) - 12G(1,1,0;y) - 2G(0,0,0;z) + 22\zeta(3)\big]\,,
\end{aligned}
$$

$$
\begin{aligned}
g_{26} = {} & -\epsilon^3\big[\zeta(2)\,G(0;x) - 3\zeta(2)\,G(-y;x) - 4\zeta(2)\,G(0;y) + 3\zeta(2)\,G(0;z) - G(0;x)\,G(0;y)\,G(0;z) \\
& + 2G(0;x)\,G(0,0;y) - G(-y;x)\,G(0,0;y) - G(0;y)\,G(0,0;x) + G(0;y)\,G(-y,0;x) \\
& + G(0;z)\,G(0,0;x) + G(0;z)\,G(0,0;y) - G(-y,0,0;x) - 3G(0,0,0;y) - \zeta(3)\big]\,,
\end{aligned}
$$

JHEP07(2022)078

$$
\begin{aligned}
g_{27} = &-5/6+\epsilon/3\big[3G(0;x)+7G(0;y)-5G(0;z)\big]-\epsilon^2/3\big[12G(0;x)G(0;y)-6G(0;x)G(0;z)\\
&-2G(0;y)G(0;z)+4G(0,0;y)-2G(0,0;z)-26\zeta(2)\big]-\epsilon^3/3\big[60\zeta(2)G(0;x)\\
&-54\zeta(2)G(-y;x)+26\zeta(2)G(0;y)-34\zeta(2)G(0;z)+6G(0;x)G(0;y)G(0;z)\\
&-12G(0;x)G(0,0;y)+6G(0;x)G(0,0;z)-18G(-y;x)G(0,0;y)-18G(0;y)G(0,0;x)\\
&+2G(0;y)G(0,0;z)+18G(0;y)G(-y,0;x)-4G(0;z)G(0,0;y)+18G(0,0,0;x)\\
&-18G(-y,0,0;x)+8G(0,0,0;y)-4G(0,0,0;z)-49\zeta(3)\big]\,,
\end{aligned}
$$

$$
g_{28} = -\epsilon^3\big[G(0,-1,0;x)-G(0,-1,-1;x)\big]\,,
$$

$$
g_{29} = \epsilon^3 G(0,1,0;y)\,,
$$

$$
g_{30} = 0\,,
$$

$$
\begin{aligned}
g_{31} = &\epsilon^2\big[G(-1;x)G(0;z)-G(0,-1;x)\big]-\epsilon^3\big[4\zeta(2)G(-1;x)+2G(-1;x)G(0,0;z)\\
&-2G(0;z)G(0,-1;x)+4G(0;z)G(-1,-1;x)+G(-1,0,0;x)+2G(0,0,-1;x)\\
&-3G(-1,0,-1;x)-4G(0,-1,-1;x)\big]\,,
\end{aligned}
$$

$$
\begin{aligned}
g_{32} = &\epsilon^3\big[2\zeta(2)G(0;x)-\zeta(2)G(-1;x)-2\zeta(2)G(0;z)+G(0;x)G(0,0;z)-G(0;z)G(0,0;x)\\
&+G(0;z)G(0,-1;x)+G(0,0,0;x)-G(-1,0,0;x)-2G(0,0,-1;x)+2G(-1,0,-1;x)\\
&-G(0,0,0;z)+\zeta(3)\big]\,,
\end{aligned}
$$

$$
g_{33} = -\epsilon^3\big[G(0;y)G(0,-1;x)-2G(0,0,-1;x)-G(0,1,0;y)\big]\,,
$$

$$
\begin{aligned}
g_{34} = &-1/4+\epsilon/2\big[2G(-1;x)+2G(0;y)-G(0;z)\big]-\epsilon^2/2\big[8G(-1;x)G(0;y)-4G(-1;x)G(0;z)\\
&-8G(0,-1;x)+8G(-1,-1;x)+4G(0,0;y)-4G(1,0;y)-2G(0,0;z)-3\zeta(2)\big]\\
&-\epsilon^3\big[6\zeta(2)G(-1;x)-4\zeta(2)G(1;y)+3\zeta(2)G(0;z)-8G(-1;x)G(0,0;y)\\
&+8G(-1;x)G(1,0;y)+4G(-1;x)G(0,0;z)-8G(-y;x)G(1,0;y)+6G(0;y)G(0,-1;x)\\
&-16G(0;y)G(-1,-1;x)+8G(0;y)G(-y,-1;x)-6G(0;z)G(0,-1;x)\\
&+8G(0;z)G(-1,-1;x)-6G(0,0,-1;x)+16G(-1,0,-1;x)+16G(0,-1,-1;x)\\
&-16G(-1,-1,-1;x)-8G(-y,0,-1;x)-4G(0,0,0;y)+4G(1,0,0;y)-4G(0,1,0;y)\\
&+4G(1,1,0;y)+2G(0,0,0;z)-6\zeta(3)\big]\,,
\end{aligned}
$$

$$
\begin{aligned}
g_{35} = &\epsilon\big[G(0;y)-G(0;z)\big]-\epsilon^2\big[G(0;x)G(0;y)-G(0;x)G(0;z)-2G(0;y)G(0;z)+3G(0,0;y)\\
&+G(0,0;z)\big]-\epsilon^3\big[3\zeta(2)G(0;x)-3\zeta(2)G(-y;x)+8\zeta(2)G(0;y)-11\zeta(2)G(0;z)\\
&+2G(0;x)G(0;y)G(0;z)-3G(0;x)G(0,0;y)-G(-y;x)G(0,0;y)-G(0;y)G(0,0;x)\\
&+G(0;y)G(-y,0;x)+2G(0;y)G(0,0;z)+G(0,0,0;x)-G(-y,0,0;x)-3G(0,0,0;y)\\
&-4G(0,0,0;z)-12\zeta(3)\big]\,,
\end{aligned}
$$

JHEP07(2022)078

$$
\begin{aligned}
g_{36} = & -5/8+\epsilon/4\big[2G(0;x)+4G(0;y)-G(0;z)\big]-\epsilon^2/4\big[4G(0;x)G(0;y)+4G(0;y)G(0;z)\\
& -6G(0,0;z)-17\zeta(2)\big]-\epsilon^3/2\big[8\zeta(2)G(0;x)-6\zeta(2)G(-y;x)-2\zeta(2)G(0;y)\\
& +11\zeta(2)G(0;z)-2G(0;x)G(0;y)G(0;z)-2G(-y;x)G(0,0;y)+2G(0;x)G(0,0;z)\\
& -2G(0;y)G(0,0;x)+2G(0;y)G(-y,0;x)-2G(0;y)G(0,0;z)+2G(0,0,0;x)\\
& -2G(-y,0,0;x)+6G(0,0,0;z)-3\zeta(3)\big]\,,\\
g_{37} = & -1+\epsilon/2\big[3G(0;x)+3G(0;y)-2G(0;z)\big]-\epsilon^2/2\big[6G(0;x)G(0;y)-3G(0;x)G(0;z)\\
& +3G(0,0;x)-G(0,0;z)-10\zeta(2)\big]-\epsilon^3/2\big[27\zeta(2)G(0;x)-18\zeta(2)G(-y;x)-7\zeta(2)G(0;z)\\
& +3G(0;x)G(0,0;z)-6G(-y;x)G(0,0;y)-12G(0;y)G(0,0;x)+6G(0;y)G(-y,0;x)\\
& +3G(0;z)G(0,0;x)+3G(0,0,0;x)-6G(-y,0,0;x)-G(0,0,0;z)-17\zeta(3)\big]\,,\\
g_{38} = & 1/2-\epsilon/2\big[2G(0;x)-2G(-1;x)+G(0;y)-G(0;z)\big]+\epsilon^2/2\big[4G(0;x)G(0;y)\\
& -2G(0;x)G(0;z)-4G(-1;x)G(0;y)+2G(-1;x)G(0;z)+2G(0,0;x)-2G(-1,0;x)\\
& +4G(0,-1;x)-4G(-1,-1;x)-2G(0,0;y)+2G(1,0;y)-7\zeta(2)\big]+\epsilon^3/2\big[18\zeta(2)G(0;x)\\
& -6\zeta(2)G(-1;x)-12\zeta(2)G(-y;x)+2\zeta(2)G(0;y)+2\zeta(2)G(1;y)-6\zeta(2)G(0;z)\\
& +2G(0;x)G(0,0;z)+4G(-1;x)G(0,0;y)-4G(-1;x)G(1,0;y)-2G(-1;x)G(0,0;z)\\
& -4G(-y;x)G(0,0;y)+4G(-y;x)G(1,0;y)-8G(0;y)G(0,0;x)-4G(0;y)G(-y,-1;x)\\
& +4G(0;y)G(-y,0;x)-4G(0;y)G(0,-1;x)+8G(0;y)G(-1,-1;x)+4G(0;y)G(-1,0;x)\\
& +2G(0;z)G(0,0;x)-2G(0;z)G(-1,0;x)+4G(0;z)G(0,-1;x)-4G(0;z)G(-1,-1;x)\\
& +2G(0,0,0;x)+2G(-1,0,0;x)-4G(0,-1,0;x)+4G(0,0,-1;x)-4G(-y,0,0;x)\\
& +4G(-1,-1,0;x)-8G(-1,0,-1;x)-8G(0,-1,-1;x)+4G(-y,0,-1;x)\\
& +8G(-1,-1,-1;x)+4G(0,0,0;y)-4G(1,0,0;y)+2G(0,1,0;y)-2G(1,1,0;y)\\
& -2G(0,0,0;z)-9\zeta(3)\big]\,,\\
g_{39} = & -\epsilon^2G(1,0;y)-\epsilon^3\big[\zeta(2)G(1;y)-G(-y;x)G(1,0;y)-G(0;y)G(0,-1;x)+G(0,0,-1;x)\\
& -G(-y,0,-1;x)-2G(1,0,0;y)+G(0,1,0;y)-G(1,1,0;y)+G(0;y)G(-y,-1;x)\big]\,,\\
g_{40} = & -1/8+\epsilon/4\big[2G(-1;x)+2G(0;y)-G(0;z)\big]-\epsilon^2/4\big[8G(-1;x)G(0;y)-4G(-1;x)G(0;z)\\
& -6G(0,-1;x)+8G(-1,-1;x)+4G(0,0;y)-4G(1,0;y)-2G(0,0;z)-\zeta(2)\big]\\
& -\epsilon^3/2\big[2\zeta(2)G(-1;x)-2\zeta(2)G(0;y)-2\zeta(2)G(1;y)+3\zeta(2)G(0;z)-8G(-1;x)G(0,0;y)\\
& +8G(-1;x)G(1,0;y)+4G(-1;x)G(0,0;z)-6G(-y;x)G(1,0;y)+6G(0;y)G(0,-1;x)\\
& -16G(0;y)G(-1,-1;x)+6G(0;y)G(-y,-1;x)-6G(0;z)G(0,-1;x)\\
& +8G(0;z)G(-1,-1;x)-3G(0,0,-1;x)+12G(-1,0,-1;x)+12G(0,-1,-1;x)\\
& -16G(-1,-1,-1;x)-6G(-y,0,-1;x)-4G(0,0,0;y)+4G(1,0,0;y)-2G(0,1,0;y)\\
& +2G(1,1,0;y)+2G(0,0,0;z)-5\zeta(3)\big]\,,
\end{aligned}
$$

$$
\begin{aligned}
g_{41} = \epsilon^3 \big[& \zeta(2) G(0;x) + 2\zeta(2) G(-1;x) + 3\zeta(2) G(-y;x) - 6\zeta(2) G(-y/(1+y);x) - 4\zeta(2) G(0;y) \\
& + 3\zeta(2) G(0;z) - G(0;x) G(0;y) G(0;z) + G(-1;x) G(0;y) G(0;z) + 2G(0;x) G(0,0;y) \\
& - G(-1;x) G(0,0;y) + G(-1;x) G(1,0;y) + G(-y;x) G(0,0;y) - G(-y;x) G(1,0;y) \\
& - 2G(-y/(1+y);x) G(0,0;y) - G(0;y) G(0,0;x) + G(0;y) G(0,-1;x) - G(0;y) G(-y,0;x) \\
& + G(0;y) G(-y,-1;x) + 2G(0;y) G(-y/(1+y),0;x) - 2G(0;y) G(-y/(1+y),-1;x) \\
& + G(0;z) G(0,0;x) - G(0;z) G(-1,0;x) - G(0;z) G(0,-1;x) + G(0;z) G(-1,-1;x) \\
& + G(0;z) G(0,0;y) + G(-1,0,0;x) - 2G(0,-1,0;x) - G(-1,0,-1;x) + 2G(0,-1,-1;x) \\
& + G(-y,0,0;x) - G(-y,0,-1;x) - 2G(-y/(1+y),0,0;x) + 2G(-y/(1+y),-1,0;x) \\
& + 2G(-y/(1+y),0,-1;x) - 2G(-y/(1+y),-1,-1;x) - 3G(0,0,0;y) + G(0,1,0;y) - \zeta(3) \big] ,
\end{aligned}
$$

$$
\begin{aligned}
g_{42} = \epsilon^2 G(1,0;y) + \epsilon^3 \big[& 3\zeta(2) G(1;y) - G(0;x) G(1,0;y) + G(-y;x) G(1,0;y) + G(0;y) G(0,-1;x) \\
& - G(0;y) G(-y,-1;x) - G(0,0,-1;x) + G(-y,0,-1;x) - G(1,0,0;y) + G(0,1,0;y) \\
& - 3G(1,1,0;y) \big] ,
\end{aligned}
$$

$$
\begin{aligned}
g_{43} = -\epsilon^2 G(1,0;y) - \epsilon^3 \big[& 3\zeta(2) G(1;y) - G(0;x) G(1,0;y) + G(-y;x) G(1,0;y) - G(0;y) G(0,-1;x) \\
& - G(0;y) G(-y,-1;x) + 3G(0,0,-1;x) + G(-y,0,-1;x) - G(1,0,0;y) + 4G(0,1,0;y) \\
& - 3G(1,1,0;y) \big] ,
\end{aligned}
$$

$$
\begin{aligned}
g_{44} = & -5/24 + \epsilon/12 \big[6G(-1;x) + 10G(0;y) - 5G(0;z) \big] - \epsilon^2/12 \big[24G(-1;x) G(0;y) \\
& - 12G(-1;x) G(0;z) - 8G(0;y) G(0;z) - 12G(0,-1;x) + 12G(-1,-1;x) + 28G(0,0;y) \\
& - 12G(1,0;y) - 2G(0,0;z) + \zeta(2) \big] + \epsilon^3/6 \big[18\zeta(2) G(0;x) - 16\zeta(2) G(0;y) - \zeta(2) G(0;z) \\
& + 6\zeta(2) G(-1;x) - 18\zeta(2) G(-y;x) + 18\zeta(2) G(1;y) - 12G(-1;x) G(0;y) G(0;z) \\
& + 6G(0;x) G(0,0;y) - 6G(0;x) G(1,0;y) + 36G(-1;x) G(0,0;y) - 12G(-1;x) G(1,0;y) \\
& - 6G(-y;x) G(0,0;y) + 18G(-y;x) G(1,0;y) - 6G(0;y) G(0,0;x) - 4G(0;y) G(0,0;z) \\
& - 6G(0;y) G(0,-1;x) + 6G(0;y) G(-y,0;x) + 24G(0;y) G(-1,-1;x) \\
& - 18G(0;y) G(-y,-1;x) - 4G(0;z) G(0,0;y) + 12G(0;z) G(0,-1;x) \\
& - 12G(0;z) G(-1,-1;x) + 6G(0,0,0;x) - 6G(-y,0,0;x) - 6G(0,0,-1;x) \\
& - 6G(-1,0,-1;x) - 12G(0,-1,-1;x) + 18G(-y,0,-1;x) + 6G(-1,-1,-1;x) \\
& + 26G(0,0,0;y) + 6G(0,1,0;y) - 6G(1,0,0;y) - 18G(1,1,0;y) + 2G(0,0,0;z) + 32\zeta(3) \big] ,
\end{aligned}
$$

JHEP07(2022)078

$$
\begin{aligned}
g_{45} = {} & 1/6-\epsilon/6\big[3G(-1;x)+4G(0;y)-2G(0;z)\big]+\epsilon^2/6\big[12G(-1;x)G(0;y)-6G(-1;x)G(0;z)\\
& -2G(0;y)G(0;z)-9G(0,-1;x)+9G(-1,-1;x)+10G(0,0;y)-6G(1,0;y)-2G(0,0;z)\\
& -2\zeta(2)\big]-\epsilon^3/6\big[18\zeta(2)G(0;x)-6\zeta(2)G(-1;x)-18\zeta(2)G(-y;x)-14\zeta(2)G(0;y)\\
& +18\zeta(2)G(1;y)-8\zeta(2)G(0;z)-6G(-1;x)G(0;y)G(0;z)+6G(0;x)G(0,0;y)\\
& -6G(0;x)G(1,0;y)+30G(-1;x)G(0,0;y)-6G(-1;x)G(0,0;z)-18G(-1;x)G(1,0;y)\\
& -6G(-y;x)G(0,0;y)+24G(-y;x)G(1,0;y)-6G(0;y)G(0,0;x)-2G(0;y)G(0,0;z)\\
& -2G(0;z)G(0,0;y)-6G(0;y)G(0,-1;x)+12G(0;z)G(0,-1;x)+6G(0;y)G(-y,0;x)\\
& -24G(0;y)G(-y,-1;x)+36G(0;y)G(-1,-1;x)-18G(0;z)G(-1,-1;x)\\
& +6G(0,0,0;x)-6G(-y,0,0;x)+3G(0,0,-1;x)+24G(-y,0,-1;x)-27G(-1,0,-1;x)\\
& -33G(0,-1,-1;x)+27G(-1,-1,-1;x)+16G(0,0,0;y)-6G(1,0,0;y)+12G(0,1,0;y)\\
& -18G(1,1,0;y)-2G(0,0,0;z)+28\zeta(3)\big],,\\
g_{46} = {} & \epsilon^2\big[G(0,-1;x)-G(-1;x)G(0;z)\big]+\epsilon^3\big[2G(-1;x)G(0;y)G(0;z)-2G(-1;x)G(0,0;y)\\
& +2G(-1;x)G(1,0;y)-2G(-y;x)G(1,0;y)-2G(0;y)G(0,-1;x)+2G(0;y)G(-y,-1;x)\\
& -2G(0;z)G(0,-1;x)+2G(0;z)G(-1,-1;x)+G(-1,0,0;x)+4G(0,0,-1;x)\\
& -3G(-1,0,-1;x)-2G(-y,0,-1;x)-2G(0,-1,-1;x)\big]. \qquad \text{(D.1)}
\end{aligned}
$$

References

[1] S.D. Drell and T.-M. Yan, *Massive Lepton Pair Production in Hadron-Hadron Collisions at High-Energies*, *Phys. Rev. Lett.* **25** (1970) 316 [*Erratum ibid.* **25** (1970) 902] [INSPIRE].

[2] ATLAS collaboration, *Precision measurement and interpretation of inclusive W^+ , W^- and Z/γ^* production cross sections with the ATLAS detector*, *Eur. Phys. J. C* **77** (2017) 367 [arXiv:1612.03016] [INSPIRE].

[3] ATLAS collaboration, *Measurement of the W-boson mass in pp collisions at $\sqrt{s} = 7$ TeV with the ATLAS detector*, *Eur. Phys. J. C* **78** (2018) 110 [*Erratum ibid.* **78** (2018) 898] [arXiv:1701.07240] [INSPIRE].

[4] S. Camarda, J. Cuth and M. Schott, *Determination of the muonic branching ratio of the W boson and its total width via cross-section measurements at the Tevatron and LHC*, *Eur. Phys. J. C* **76** (2016) 613 [arXiv:1607.05084] [INSPIRE].

[5] ATLAS collaboration, *Measurement of the forward-backward asymmetry of electron and muon pair-production in pp collisions at $\sqrt{s} = 7$ TeV with the ATLAS detector*, *JHEP* **09** (2015) 049 [arXiv:1503.03709] [INSPIRE].

JHEP07(2022)078

[6] CMS collaboration, *Measurement of the weak mixing angle using the forward-backward asymmetry of Drell-Yan events in pp collisions at 8 TeV*, *Eur. Phys. J. C* **78** (2018) 701 [arXiv:1806.00863] [INSPIRE].

[7] CMS collaboration, *Measurement of the differential cross section and charge asymmetry for inclusive $pp \to W^{\pm} + X$ production at $\sqrt{s} = 8$ TeV*, *Eur. Phys. J. C* **76** (2016) 469 [arXiv:1603.01803] [INSPIRE].

[8] CMS collaboration, *Measurements of the W boson rapidity, helicity, double-differential cross sections, and charge asymmetry in pp collisions at $\sqrt{s} = 13$ TeV*, *Phys. Rev. D* **102** (2020) 092012 [arXiv:2008.04174] [INSPIRE].

[9] ATLAS collaboration, *Search for new resonances in events with one lepton and missing transverse momentum in pp collisions at $\sqrt{s} = 13$ TeV with the ATLAS detector*, *Phys. Lett. B* **762** (2016) 334 [arXiv:1606.03977] [INSPIRE].

[10] CMS collaboration, *Search for heavy gauge W' boson in events with an energetic lepton and large missing transverse momentum at $\sqrt{s} = 13$ TeV*, *Phys. Lett. B* **770** (2017) 278 [arXiv:1612.09274] [INSPIRE].

[11] ATLAS collaboration, *Search for a new heavy gauge boson resonance decaying into a lepton and missing transverse momentum in 36 fb^{-1} of pp collisions at $\sqrt{s} = 13$ TeV with the ATLAS experiment*, *Eur. Phys. J. C* **78** (2018) 401 [arXiv:1706.04786] [INSPIRE].

[12] ATLAS collaboration, *Search for a heavy charged boson in events with a charged lepton and missing transverse momentum from pp collisions at $\sqrt{s} = 13$ TeV with the ATLAS detector*, *Phys. Rev. D* **100** (2019) 052013 [arXiv:1906.05609] [INSPIRE].

[13] ATLAS collaboration, *Search for high-mass new phenomena in the dilepton final state using proton-proton collisions at $\sqrt{s} = 13$ TeV with the ATLAS detector*, *Phys. Lett. B* **761** (2016) 372 [arXiv:1607.03669] [INSPIRE].

[14] CMS collaboration, *Search for narrow resonances in dilepton mass spectra in proton-proton collisions at $\sqrt{s} = 13$ TeV and combination with 8 TeV data*, *Phys. Lett. B* **768** (2017) 57 [arXiv:1609.05391] [INSPIRE].

[15] ATLAS collaboration, *Search for high-mass dilepton resonances using 139 fb^{-1} of pp collision data collected at $\sqrt{s} = 13$ TeV with the ATLAS detector*, *Phys. Lett. B* **796** (2019) 68 [arXiv:1903.06248] [INSPIRE].

[16] G. Altarelli, R.K. Ellis and G. Martinelli, *Large Perturbative Corrections to the Drell-Yan Process in QCD*, *Nucl. Phys. B* **157** (1979) 461 [INSPIRE].

[17] T. Matsuura, S.C. van der Marck and W.L. van Neerven, *The Calculation of the Second Order Soft and Virtual Contributions to the Drell-Yan Cross-Section*, *Nucl. Phys. B* **319** (1989) 570 [INSPIRE].

[18] R. Hamberg, W.L. van Neerven and T. Matsuura, *A complete calculation of the order α_s^2 correction to the Drell-Yan K-factor*, *Nucl. Phys. B* **359** (1991) 343 [*Erratum ibid.* **644** (2002) 403] [INSPIRE].

[19] R.V. Harlander and W.B. Kilgore, *Next-to-next-to-leading order Higgs production at hadron colliders*, *Phys. Rev. Lett.* **88** (2002) 201801 [hep-ph/0201206] [INSPIRE].

[20] C. Anastasiou, L.J. Dixon, K. Melnikov and F. Petriello, *High precision QCD at hadron colliders: Electroweak gauge boson rapidity distributions at NNLO*, *Phys. Rev. D* **69** (2004) 094008 [hep-ph/0312266] [INSPIRE].

JHEP07(2022)078

[21] K. Melnikov and F. Petriello, *The W boson production cross section at the LHC through $O(\alpha_s^2)$*, *Phys. Rev. Lett.* **96** (2006) 231803 [hep-ph/0603182] [INSPIRE].

[22] K. Melnikov and F. Petriello, *Electroweak gauge boson production at hadron colliders through $O(\alpha_s^2)$*, *Phys. Rev. D* **74** (2006) 114017 [hep-ph/0609070] [INSPIRE].

[23] S. Catani, L. Cieri, G. Ferrera, D. de Florian and M. Grazzini, *Vector boson production at hadron colliders: a fully exclusive QCD calculation at NNLO*, *Phys. Rev. Lett.* **103** (2009) 082001 [arXiv:0903.2120] [INSPIRE].

[24] S. Catani, G. Ferrera and M. Grazzini, *W Boson Production at Hadron Colliders: The Lepton Charge Asymmetry in NNLO QCD*, *JHEP* **05** (2010) 006 [arXiv:1002.3115] [INSPIRE].

[25] T. Ahmed, M. Mahakhud, N. Rana and V. Ravindran, *Drell-Yan Production at Threshold to Third Order in QCD*, *Phys. Rev. Lett.* **113** (2014) 112002 [arXiv:1404.0366] [INSPIRE].

[26] T. Ahmed, M.K. Mandal, N. Rana and V. Ravindran, *Rapidity Distributions in Drell-Yan and Higgs Productions at Threshold to Third Order in QCD*, *Phys. Rev. Lett.* **113** (2014) 212003 [arXiv:1404.6504] [INSPIRE].

[27] C. Duhr, F. Dulat and B. Mistlberger, *Drell-Yan Cross Section to Third Order in the Strong Coupling Constant*, *Phys. Rev. Lett.* **125** (2020) 172001 [arXiv:2001.07717] [INSPIRE].

[28] C. Duhr, F. Dulat and B. Mistlberger, *Charged current Drell-Yan production at N^3LO*, *JHEP* **11** (2020) 143 [arXiv:2007.13313] [INSPIRE].

[29] C. Duhr and B. Mistlberger, *Lepton-pair production at hadron colliders at N^3LO in QCD*, *JHEP* **03** (2022) 116 [arXiv:2111.10379] [INSPIRE].

[30] S. Camarda, L. Cieri and G. Ferrera, *Drell-Yan lepton-pair production: q_T resummation at N^3LL accuracy and fiducial cross sections at N^3LO*, *Phys. Rev. D* **104** (2021) L111503 [arXiv:2103.04974] [INSPIRE].

[31] X. Chen, T. Gehrmann, N. Glover, A. Huss, T.-Z. Yang and H.X. Zhu, *Dilepton Rapidity Distribution in Drell-Yan Production to Third Order in QCD*, *Phys. Rev. Lett.* **128** (2022) 052001 [arXiv:2107.09085] [INSPIRE].

[32] U. Baur, S. Keller and W.K. Sakumoto, *QED radiative corrections to Z boson production and the forward backward asymmetry at hadron colliders*, *Phys. Rev. D* **57** (1998) 199 [hep-ph/9707301] [INSPIRE].

[33] U. Baur, O. Brein, W. Hollik, C. Schappacher and D. Wackeroth, *Electroweak radiative corrections to neutral current Drell-Yan processes at hadron colliders*, *Phys. Rev. D* **65** (2002) 033007 [hep-ph/0108274] [INSPIRE].

[34] V.A. Zykunov, *Radiative corrections to the Drell-Yan process at large dilepton invariant masses*, *Phys. Atom. Nucl.* **69** (2006) 1522 [INSPIRE].

[35] V.A. Zykunov, *Weak radiative corrections to Drell-Yan process for large invariant mass of di-lepton pair*, *Phys. Rev. D* **75** (2007) 073019 [hep-ph/0509315] [INSPIRE].

[36] C.M. Carloni Calame, G. Montagna, O. Nicrosini and A. Vicini, *Precision electroweak calculation of the production of a high transverse-momentum lepton pair at hadron colliders*, *JHEP* **10** (2007) 109 [arXiv:0710.1722] [INSPIRE].

[37] A. Arbuzov et al., *One-loop corrections to the Drell-Yan process in SANC. (II). The Neutral current case*, *Eur. Phys. J. C* **54** (2008) 451 [arXiv:0711.0625] [INSPIRE].

JHEP07(2022)078

[38] S. Dittmaier and M. Huber, *Radiative corrections to the neutral-current Drell-Yan process in the Standard Model and its minimal supersymmetric extension*, *JHEP* **01** (2010) 060 [arXiv:0911.2329] [INSPIRE].

[39] D. Wackeroth and W. Hollik, *Electroweak radiative corrections to resonant charged gauge boson production*, *Phys. Rev. D* **55** (1997) 6788 [hep-ph/9606398] [INSPIRE].

[40] U. Baur, S. Keller and D. Wackeroth, *Electroweak radiative corrections to W boson production in hadronic collisions*, *Phys. Rev. D* **59** (1999) 013002 [hep-ph/9807417] [INSPIRE].

[41] S. Dittmaier and M. Krämer, *Electroweak radiative corrections to W boson production at hadron colliders*, *Phys. Rev. D* **65** (2002) 073007 [hep-ph/0109062] [INSPIRE].

[42] U. Baur and D. Wackeroth, *Electroweak radiative corrections to $p\bar{p} \to W^{\pm} \to \ell^{\pm}\nu$ beyond the pole approximation*, *Phys. Rev. D* **70** (2004) 073015 [hep-ph/0405191] [INSPIRE].

[43] A. Arbuzov et al., *One-loop corrections to the Drell-Yan process in SANC. I. The Charged current case*, *Eur. Phys. J. C* **46** (2006) 407 [*Erratum ibid.* **50** (2007) 505] [hep-ph/0506110] [INSPIRE].

[44] C.M. Carloni Calame, G. Montagna, O. Nicrosini and A. Vicini, *Precision electroweak calculation of the charged current Drell-Yan process*, *JHEP* **12** (2006) 016 [hep-ph/0609170] [INSPIRE].

[45] S. Brensing, S. Dittmaier, M. Krämer and A. Muck, *Radiative corrections to W^- boson hadroproduction: Higher-order electroweak and supersymmetric effects*, *Phys. Rev. D* **77** (2008) 073006 [arXiv:0710.3309] [INSPIRE].

[46] S. Alioli et al., *Precision studies of observables in $pp \to W \to l\nu_l$ and $pp \to \gamma, Z \to l^+l^-$ processes at the LHC*, *Eur. Phys. J. C* **77** (2017) 280 [arXiv:1606.02330] [INSPIRE].

[47] y S. Alioli, C.W. Bauer, C. Berggren, F.J. Tackmann and J.R. Walsh, *Drell-Yan production at NNLL'+NNLO matched to parton showers*, *Phys. Rev. D* **92** (2015) 094020 [arXiv:1508.01475] [INSPIRE].

[48] S. Alioli, C.W. Bauer, S. Guns and F.J. Tackmann, *Underlying event sensitive observables in Drell-Yan production using GENEVA*, *Eur. Phys. J. C* **76** (2016) 614 [arXiv:1605.07192] [INSPIRE].

[49] S. Camarda et al., *DYTurbo: Fast predictions for Drell-Yan processes*, *Eur. Phys. J. C* **80** (2020) 251 [*Erratum ibid.* **80** (2020) 440] [arXiv:1910.07049] [INSPIRE].

[50] R. Boughezal et al., *Color singlet production at NNLO in MCFM*, *Eur. Phys. J. C* **77** (2017) 7 [arXiv:1605.08011] [INSPIRE].

[51] M. Grazzini, S. Kallweit and M. Wiesemann, *Fully differential NNLO computations with MATRIX*, *Eur. Phys. J. C* **78** (2018) 537 [arXiv:1711.06631] [INSPIRE].

[52] P.F. Monni, P. Nason, E. Re, M. Wiesemann and G. Zanderighi, *MiNNLO$_{PS}$: a new method to match NNLO QCD to parton showers*, *JHEP* **05** (2020) 143 [arXiv:1908.06987] [INSPIRE].

[53] S. Alekhin, A. Kardos, S. Moch and Z. Trócsányi, *Precision studies for Drell-Yan processes at NNLO*, *Eur. Phys. J. C* **81** (2021) 573 [arXiv:2104.02400] [INSPIRE].

[54] D. de Florian, M. Der and I. Fabre, *QCD $\oplus$ QED NNLO corrections to Drell-Yan production*, *Phys. Rev. D* **98** (2018) 094008 [arXiv:1805.12214] [INSPIRE].

JHEP07(2022)078

[55] M. Delto, M. Jaquier, K. Melnikov and R. Röntsch, *Mixed QCD ⊗ QED corrections to on-shell Z boson production at the LHC*, *JHEP* **01** (2020) 043 [arXiv:1909.08428] [INSPIRE].

[56] L. Cieri, D. de Florian, M. Der and J. Mazzitelli, *Mixed QCD ⊗ QED corrections to exclusive Drell-Yan production using the q_T -subtraction method*, *JHEP* **09** (2020) 155 [arXiv:2005.01315] [INSPIRE].

[57] R. Bonciani, F. Buccioni, N. Rana, I. Triscari and A. Vicini, *NNLO QCD × EW corrections to Z production in the $q\bar{q}$ channel*, *Phys. Rev. D* **101** (2020) 031301 [arXiv:1911.06200] [INSPIRE].

[58] F. Buccioni, F. Caola, M. Delto, M. Jaquier, K. Melnikov and R. Röntsch, *Mixed QCD-electroweak corrections to on-shell Z production at the LHC*, *Phys. Lett. B* **811** (2020) 135969 [arXiv:2005.10221] [INSPIRE].

[59] R. Bonciani, F. Buccioni, N. Rana and A. Vicini, *Next-to-Next-to-Leading Order Mixed QCD-Electroweak Corrections to on-Shell Z Production*, *Phys. Rev. Lett.* **125** (2020) 232004 [arXiv:2007.06518] [INSPIRE].

[60] A. Behring et al., *Mixed QCD-electroweak corrections to W-boson production in hadron collisions*, *Phys. Rev. D* **103** (2021) 013008 [arXiv:2009.10386] [INSPIRE].

[61] S. Dittmaier, T. Schmidt and J. Schwarz, *Mixed NNLO QCD-electroweak corrections of $\mathcal{O}(N_f\alpha_s\alpha)$ to single-W/Z production at the LHC*, *JHEP* **12** (2020) 201 [arXiv:2009.02229] [INSPIRE].

[62] S. Dittmaier, A. Huss and C. Schwinn, *Mixed QCD-electroweak $\mathcal{O}(\alpha_s\alpha)$ corrections to Drell-Yan processes in the resonance region: pole approximation and non-factorizable corrections*, *Nucl. Phys. B* **885** (2014) 318 [arXiv:1403.3216] [INSPIRE].

[63] S. Dittmaier, A. Huss and C. Schwinn, *Dominant mixed QCD-electroweak $O(\alpha_s\alpha)$ corrections to Drell-Yan processes in the resonance region*, *Nucl. Phys. B* **904** (2016) 216 [arXiv:1511.08016] [INSPIRE].

[64] L. Buonocore, M. Grazzini, S. Kallweit, C. Savoini and F. Tramontano, *Mixed QCD-EW corrections to $pp \to \ell\nu_\ell + X$ at the LHC*, *Phys. Rev. D* **103** (2021) 114012 [arXiv:2102.12539] [INSPIRE].

[65] R. Bonciani, S. Di Vita, P. Mastrolia and U. Schubert, *Two-Loop Master Integrals for the mixed EW-QCD virtual corrections to Drell-Yan scattering*, *JHEP* **09** (2016) 091 [arXiv:1604.08581] [INSPIRE].

[66] A. von Manteuffel and R.M. Schabinger, *Numerical Multi-Loop Calculations via Finite Integrals and One-Mass EW-QCD Drell-Yan Master Integrals*, *JHEP* **04** (2017) 129 [arXiv:1701.06583] [INSPIRE].

[67] M. Heller, A. von Manteuffel and R.M. Schabinger, *Multiple polylogarithms with algebraic arguments and the two-loop EW-QCD Drell-Yan master integrals*, *Phys. Rev. D* **102** (2020) 016025 [arXiv:1907.00491] [INSPIRE].

[68] M. Heller, A. von Manteuffel, R.M. Schabinger and H. Spiesberger, *Mixed EW-QCD two-loop amplitudes for $q\bar{q} \to \ell^+\ell^-$ and γ_5 scheme independence of multi-loop corrections*, *JHEP* **05** (2021) 213 [arXiv:2012.05918] [INSPIRE].

[69] T. Armadillo, R. Bonciani, S. Devoto, N. Rana and A. Vicini, *Two-loop mixed QCD-EW corrections to neutral current Drell-Yan*, *JHEP* **05** (2022) 072 [arXiv:2201.01754] [INSPIRE].

JHEP07(2022)078

[70] R. Bonciani et al., *Mixed Strong-Electroweak Corrections to the Drell-Yan Process*, *Phys. Rev. Lett.* **128** (2022) 012002 [arXiv:2106.11953] [INSPIRE].

[71] F. Buccioni et al., *Mixed QCD-electroweak corrections to dilepton production at the LHC in the high invariant mass region*, *JHEP* **06** (2022) 022 [arXiv:2203.11237] [INSPIRE].

[72] T. Kinoshita, *Mass singularities of Feynman amplitudes*, *J. Math. Phys.* **3** (1962) 650 [INSPIRE].

[73] T.D. Lee and M. Nauenberg, *Degenerate Systems and Mass Singularities*, *Phys. Rev.* **133** (1964) B1549 [INSPIRE].

[74] S.M. Hasan and U. Schubert, *Master Integrals for the mixed QCD-QED corrections to the Drell-Yan production of a massive lepton pair*, *JHEP* **11** (2020) 107 [arXiv:2004.14908] [INSPIRE].

[75] D. Binosi, J. Collins, C. Kaufhold and L. Theussl, *JaxoDraw: A Graphical user interface for drawing Feynman diagrams. Version 2.0 release notes*, *Comput. Phys. Commun.* **180** (2009) 1709 [arXiv:0811.4113] [INSPIRE].

[76] K.G. Chetyrkin and F.V. Tkachov, *Integration by Parts: The Algorithm to Calculate β-functions in 4 Loops*, *Nucl. Phys. B* **192** (1981) 159 [INSPIRE].

[77] A.V. Kotikov, *Differential equations method: New technique for massive Feynman diagrams calculation*, *Phys. Lett. B* **254** (1991) 158 [INSPIRE].

[78] E. Remiddi, *Differential equations for Feynman graph amplitudes*, *Nuovo Cim. A* **110** (1997) 1435 [hep-th/9711188] [INSPIRE].

[79] P. Maierhöfer, J. Usovitsch and P. Uwer, *Kira — A Feynman integral reduction program*, *Comput. Phys. Commun.* **230** (2018) 99 [arXiv:1705.05610] [INSPIRE].

[80] J. Klappert, F. Lange, P. Maierhöfer and J. Usovitsch, *Integral reduction with Kira 2.0 and finite field methods*, *Comput. Phys. Commun.* **266** (2021) 108024 [arXiv:2008.06494] [INSPIRE].

[81] S. Laporta, *High precision calculation of multiloop Feynman integrals by difference equations*, *Int. J. Mod. Phys. A* **15** (2000) 5087 [hep-ph/0102033] [INSPIRE].

[82] R.N. Lee, *Presenting LiteRed: a tool for the Loop InTEgrals REDuction*, arXiv:1212.2685 [INSPIRE].

[83] R.N. Lee, *LiteRed 1.4: a powerful tool for reduction of multiloop integrals*, *J. Phys. Conf. Ser.* **523** (2014) 012059 [arXiv:1310.1145] [INSPIRE].

[84] J.M. Henn, *Multiloop integrals in dimensional regularization made simple*, *Phys. Rev. Lett.* **110** (2013) 251601 [arXiv:1304.1806] [INSPIRE].

[85] A.B. Goncharov, *Multiple polylogarithms and mixed Tate motives*, math/0103059 [INSPIRE].

[86] A.B. Goncharov, *Multiple polylogarithms, cyclotomy and modular complexes*, *Math. Res. Lett.* **5** (1998) 497 [arXiv:1105.2076] [INSPIRE].

[87] D. Maître, *HPL, a mathematica implementation of the harmonic polylogarithms*, *Comput. Phys. Commun.* **174** (2006) 222 [hep-ph/0507152] [INSPIRE].

[88] D. Maître, *Extension of HPL to complex arguments*, *Comput. Phys. Commun.* **183** (2012) 846 [hep-ph/0703052] [INSPIRE].

[89] C. Duhr and F. Dulat, *PolyLogTools — polylogs for the masses*, *JHEP* **08** (2019) 135 [arXiv:1904.07279] [INSPIRE].

JHEP07(2022)078

[90] C.W. Bauer, A. Frink and R. Kreckel, *Introduction to the GiNaC framework for symbolic computation within the C++ programming language*, *J. Symb. Comput.* **33** (2002) 1 [cs/0004015].

[91] J. Vollinga and S. Weinzierl, *Numerical evaluation of multiple polylogarithms*, *Comput. Phys. Commun.* **167** (2005) 177 [hep-ph/0410259] [INSPIRE].

[92] P. Mastrolia, M. Passera, A. Primo and U. Schubert, *Master integrals for the NNLO virtual corrections to μe scattering in QED: the planar graphs*, *JHEP* **11** (2017) 198 [arXiv:1709.07435] [INSPIRE].

[93] S. Borowka et al., *pySecDec: a toolbox for the numerical evaluation of multi-scale integrals*, *Comput. Phys. Commun.* **222** (2018) 313 [arXiv:1703.09692] [INSPIRE].

[94] S. Borowka, G. Heinrich, S. Jahn, S.P. Jones, M. Kerner and J. Schlenk, *A GPU compatible quasi-Monte Carlo integrator interfaced to pySecDec*, *Comput. Phys. Commun.* **240** (2019) 120 [arXiv:1811.11720] [INSPIRE].

[95] T. Gehrmann, A. von Manteuffel, L. Tancredi and E. Weihs, *The two-loop master integrals for $q\bar{q} \to VV$*, *JHEP* **06** (2014) 032 [arXiv:1404.4853] [INSPIRE].

[96] E. Panzer, *Algorithms for the symbolic integration of hyperlogarithms with applications to Feynman integrals*, *Comput. Phys. Commun.* **188** (2015) 148 [arXiv:1403.3385] [INSPIRE].

[97] A. Pak and A. Smirnov, *Geometric approach to asymptotic expansion of Feynman integrals*, *Eur. Phys. J. C* **71** (2011) 1626 [arXiv:1011.4863] [INSPIRE].

[98] B. Jantzen, A.V. Smirnov and V.A. Smirnov, *Expansion by regions: revealing potential and Glauber regions automatically*, *Eur. Phys. J. C* **72** (2012) 2139 [arXiv:1206.0546] [INSPIRE].

[99] A.V. Smirnov, *FIESTA4: Optimized Feynman integral calculations with GPU support*, *Comput. Phys. Commun.* **204** (2016) 189 [arXiv:1511.03614] [INSPIRE].

[100] A.V. Smirnov, N.D. Shapurov and L.I. Vysotsky, *FIESTA5: Numerical high-performance Feynman integral evaluation*, *Comput. Phys. Commun.* **277** (2022) 108386 [arXiv:2110.11660] [INSPIRE].

JHEP07(2022)078